This is a preprint draft. The published article can be found at: https://doi.org/10.1007/s10694-022-01290-7.

Please cite this paper as:

Tapeh, A., Naser, M.Z. (2022). Discovering Graphical Heuristics on Fire-induced Spalling of Concrete through eXplainable Artificial Intelligence. *Fire Technology*. https://doi.org/10.1007/s10694-022-01290-7.

Discovering Graphical Heuristics on Fire-induced Spalling of Concrete through eXplainable Artificial Intelligence

Arash Teymori Gharah Tapeh[1], M.Z. Naser[2, 3]

[1]Graduate Student, School of Civil & Environmental Engineering and Earth Sciences (SCEEES), Clemson University, USA

E-mail: teymouriarash89@gmail.com

[2]Assistant Professor, School of Civil & Environmental Engineering and Earth Sciences (SCEEES), Clemson University, USA

[3]Artificial Intelligence Research Institute for Science and Engineering (AIRISE), Clemson University, Clemson, SC, USA

E-mail: mznaser@clemson.edu, Website: www.mznaser.com

Abstract

Fire-induced spalling of concrete continues to be an intriguing and intricate research problem. A deep dive into the open literature highlights the alarming discrepancy and inconsistency of existing theories, as well as the complexity of predicting spalling. This brings new challenges to creating fire-safe concretes and primes an opportunity to explore modern methods of investigation to tackle the spalling phenomenon. Thus, this paper leverages the latest advancements in eXplainable Artificial Intelligence (XAI) to vet existing theories on fire-induced spalling and to discover solutions/heuristics to predict spalling of concrete mixtures. The developed heuristics are in the form of *graphs* and *nomograms*. The proposed solutions allow interested researchers and engineers to graphically identify the propensity of a given concrete mixture to spalling directly and with ease. For example, we report that concrete mixtures with a combination of moderate water/binder ratio (of about 0.3), low heating rate (less than 2.5ºC/min), moderate rise in temperature (less than 500ºC), and have moisture content (less than 3%) are expected to be less prone to spalling. Further, findings from this research showcase the potential for developing simple (i.e., one-shot) and graphical (coding-free and formula-free) XAI-based solutions and web applications to address decades-long problems in the area of concrete research.

Keywords: Explainable Artificial Intelligence, Fire, Concrete, Spalling, Nomogram.

1.0 Introduction

Concrete is one of the most widely used construction materials. A prime quality of concrete lies within its inert material properties that often lead to favorable performance at elevated temperatures [1,2]. Nonetheless, it is common for concrete to undergo varying degrees of damage under fire conditions. Such damage can be attributed to thermo-chemical-mechanical degradations triggered by the rise in temperature [3]. The severity of the noted changes is governed by the multitude and proportions of raws (i.e., aggregates, sand, water, admixtures, etc.) making up the concrete mixture and fire characteristics, to name a few. For example, each raw material responds differently to the rise in temperature, and the interaction of these materials also reacts uniquely to the same temperature rise and heating rate [4]. These processes can trigger fire-induced spalling.

The *spalling phenomenon* is often defined as the *disintegration/flaking of concrete chunks from the sides or surfaces of sections or members* [5]. Spalling can occur in a mild or explosive nature. The degree at which spalling takes place can be a function of a variety of conditions (heating rate, maximum temperature, etc.) as well as mixture properties (water content, types of raws, etc.), among other factors. As one expects, the breakout of concrete pieces under fire conditions can lead to: 1) a reduction in the size (i.e., cross-section) of the element, 2) directly exposing internal reinforcements (namely: steel reinforcement, prestressing strands, or fiber-reinforced polymer composites) and inner layers of concrete to fire, and 3) flame propagation through cracks in barrier elements (such as walls, and slabs). The combined effect of the above three actions implies that spalling can accelerate damage and failure in spalling-prone concrete structures [6,7]. It is also noteworthy to mention that the adverse effect of spalling can have a compound effect on the geometric features of a concrete element (i.e., at the mechanical level and the thermal propagation)[1].

Notable and recent works have reported that traditional and modern concretes (such as those of high strength and/or ultra high-strength characteristics) can be prone to spalling [7–11]. Spalling amplifies in modern concretes due to the complex chemicals/additives involved in preparing such mixtures and their resulting denser microstructure [12,13]. Holistically, fire-induced spalling can be attributed to three temperature-dependent/temperature-triggered mechanisms: 1) rise in pore vapor pressure, 2) generated thermal stresses, and 3) combined pore pressure and thermal stresses [10]. Spalling could also be classified into three different groups depending on its occurrence. For instance, spalling could occur during the early-stage (220-230°C), mid-stage (430-660°C), and late-stage (above 700°C) of fires. Please refer to [3,4] for a more thorough discussion on spalling mechanisms.

While the literature on fire-induced spalling is rich, as noted by the above-cited works and others [14–19], we still lack a fundamental and consistent testing procedure to predict if a concrete mixture is prone to spalling. In parallel, we also lack a consistent computational approach to predict if spalling will occur or not. This could be partly attributed to the 1) complexity in testing for spalling, 2) the variety of existing concrete mixtures, 3) the discrepancy in proposed test methodologies, and 4) the difficulty of repeating published results[2].

In parallel, many of the existing codal provisions remain impartial to the problem of spalling and provide general recommendations intended for this phenomenon [20,21]. These provisions often assume that spalling does not occur or, if it does, to be of a negligible impact. This assumption jeopardizes the applicability of established requirements in the event of spalling (i.e., tabulated data for assigning fire resistance rating of concrete members, etc.). The surveyed literature above

[1] We thank Reviewer no. 2 for pointing out this compound effect.

[2] It is worth acknowledging the impressive work led by RILEM on this front.

reminds us of how predicting spalling can be a hectic process. These complications, along with others, have also been echoed by our colleagues [22–26].

To overcome the limitations of fire testing or fire-based simulations in capturing the spalling phenomenon, the rise of big data and artificial intelligence (AI) provides an attractive approach that could be able to tackle this phenomenon. In this frontier, emphasis is placed on creating AI models capable of analyzing observations from fire tests to capture possible patterns of spalling. The core hypothesis herein is that it could be possible to identify commonalities in which concrete spalls through a data-driven analysis instead of a traditional analysis. While such an approach *may* not fully unveil the mechanisms of how spalling occurs, it can still provide us with 1) new knowledge that could help us arrive at such mechanisms or 2) rules of thumb (heuristics) that can come in handy to develop timely solutions [27]. These two possibilities are the motivation behind this work.

Although serious efforts aimed at integrating AI into our domain are relatively new, the open literature documents early works that explored AI as a means to predict spalling. For instance, Uysal and Tanyildizi [28] and McKinney and Ali [29] are perhaps some of the earliest works that tackled the spalling problem through AI. More recently, the use of modern algorithms and techniques has also been tried by our research group [5,12,29–31] and colleagues [32–34]. In hindsight, these recent studies examine the vulnerability of concrete elements or concrete mixes to spalling via investigating the influence of *elemental features* (such as geometrical, materials, and loading properties of load bearing members) or *concrete mixtures* (e.g., proportions of aggregates, sand, binders, etc.).

Much of the cited works on the AI front, except [35], applied blackbox AI. In such AI, the logic and rationale behind models' predictions are opaque. In other words, the user does not know how and why a model arrives at a specific prediction nor how the model ties the inputs (features) to the output (phenomenon) in question. As one can expect, blackbox models resemble a crude data-driven approach where the data and model architecture dictate the resulting predictions with little physics-informed knowledge on such a procedure. While such an approach can be useful for developing *practical* data-driven solutions, it may remain limited to unlocking the spalling mechanism(s).

In pursuit of more transparent AI, recent advances have led to producing AI models that are eXplainable (and hence the term XAI) [36,37]. In XAI, each model can demonstrate how the input features were forged into arriving at a prediction and which feature(s) govern the predictivity of the model. Through XAI, while still confined within the data-driven realm, a user can arrive at valuable insights into how the model has utilized the data (e.g., observations from fire tests on spalling) to arrive at accurate predictions[3]. These insights can then be leveraged to develop possible rules of thumb to address our problems. It is also likely that the same insights can be directed to

[3] Please refer to our philosophical discussion on AI and XAI [92].

identify directions of high merit in research and future experiments – see a relevant example pertaining to the COVID-19 pandemic [38].

In lieu of attaining insights from XAI, one can also derive graphical solutions (heuristics) for our problems. Such heuristics can be formed from XAI insights or a traditional AI analysis through *nomograms*[4]; wherein the relationship between the inputs is obtained (explicitly by XAI, or implicitly by AI), and then these relationships are visually represented within a nomogram. The goal of nomograms is to accelerate routine calculations often belonging to complex and iterative problems. Most nomograms encompass *n* scales, each representing one variable in a given or considered phenomenon. Thus, when the values of *n-1* variables are obtained, a user can graphically arrive at the last unknown variable (often the dependent variable or outcome). More specifically, a nomogram can be directly used to predict the problem on hand (i.e., the occurrence of spalling) without requiring a lengthy/iterative procedure or re-running an AI/XAI analysis. Interested readers are advised to review the following works for an in-depth discussion on nomography [39–41].

This study aims to chart a path to discovering graphical heuristics and nomograms to predict fire-induced concrete spalling through XAI and AI. In this quest, 293 observations from fire tests were collected from the open literature to investigate the phenomenon of fire-induced spalling in concrete. Two approaches are used to analyze this data, through XAI models (where explainability is arrived at through the SHAP method [42] and partial dependence plots [43]) and via a nomogram obtained from an AI-based analysis. Our findings indicate that insights from XAI and AI-based nomograms can yield highly accurate and robust predictions of fire-induced spalling of concrete.

2.0 Data Collection and Methodology

2.1 Dataset development and statistical details

A database containing 293 laboratory samples was collected from the open literature [32–34,44–66]. This 293 data point sample contains 11 independent variables and one dependent variable (output; classified as spalling/no spalling). The input variables include (water/binder ratio, silica fume/binder ratio, fly ash/binder ratio, GGBS[5]/binder ratio, fine aggregate/binder ratio, coarse aggregate/binder ratio, moisture content, heating rate, maximum exposure temperature, maximum aggregate size, and the characteristic length (or distance)[6]). These inputs are used to classify and predict the occurrence of spalling in concrete as a function of the mixture proportions. It is worth noting that raw proportions were kept as a ratio of the binder for simplicity and consistency.

[4] A nomogram, also called nomograph or alignment chart, is a two-dimensional graphical calculator invented in the 19th century by the French engineer Philbert d'Ocagne to represent mathematical expressions or laws. Nomograms have been heavily utilized in engineering and medical problems [93–100].

[5] GGBS: Ground granulated blast-furnace slag.

[6] Characteristic length is defined by [33] as the distance of shortest escape route of vapor from the specimen centroid to the specimen surface.

This is a preprint draft. The published article can be found at: https://doi.org/10.1007/s10694-022-01290-7.

Please cite this paper as:

Tapeh, A., Naser, M.Z. (2022). Discovering Graphical Heuristics on Fire-induced Spalling of Concrete through eXplainable Artificial Intelligence. *Fire Technology*. https://doi.org/10.1007/s10694-022-01290-7.

Table 1 shows a statistical analysis of the dataset. As one can be seen, the database has a balanced and healthy range of all the identified variables. The result of a Pearson correlation analysis (which examines the *linear* relationship between the features and features and output) is also listed in Table 1. This correlation matrix shows that there is a positive linear correlation between *H*, *M*, *D*, *T*, *Sf/b*, *Agg*, *G/b*, and the propensity to spalling, and a negative correlation between the other features and spalling. Overall, the calculated linear correlation seems to vary between weak and mediocre, with the largest correlation arising between *T* and spalling propensity.

To compliment the Pearson correlation analysis, the Spearman and mutual information analyses are also presented. The former examines the monotonic relationship between variables, while the latter measures the reduction of uncertainty in one variable after observing another variable. It is clear that there is a good convergence between the Person and Spearman correlations. On the other hand, the mutual information analysis shows minor information exchange between the propensity of spalling and mixture components. We suspect that the actual relations between the features to be of a nonlinear form – as will be seen in a later section.

This is a preprint draft. The published article can be found at: https://doi.org/10.1007/s10694-022-01290-7.

Please cite this paper as:

Tapeh, A., Naser, M.Z. (2022). Discovering Graphical Heuristics on Fire-induced Spalling of Concrete through eXplainable Artificial Intelligence. *Fire Technology*. https://doi.org/10.1007/s10694-022-01290-7.

154 Table 1 Statistical details of the database as well as the correlation matrix

Input variables	Mean	Median	Standard Deviation	Minimum	Maximum	Skewness
Water/binder (*W/b*)	0.37	0.33	0.12	0.19	0.61	0.42
Coarse aggregate/binder (*Ca/b*)	1.73	1.77	0.90	0.00	3.95	0.10
Fine aggregate/binder ratio (*Fa/b*)	1.65	1.51	0.65	0.45	3.38	0.79
Heating rate (*H*, °C/min)	28.55	5.00	42.02	0.25	240	1.78
Moisture content of concrete (*M*)	0.03	0.04	0.020	0.00	0.07	-0.38
Characteristic distance of the concrete (*D*)	61.91	50.00	37.60	20.00	200.00	2.08
Maximum exposure temperature (T_{max}, °C)	568.20	600.00	246.20	100.00	1200.00	0.22
Silica fume/binder (*Sf/b*)	0.03	0.00	0.06	0.00	0.20	1.66
Maximum size of aggregate (*Sa*)	12.76	13.00	6.60	0.12	32.00	0.18
GGBS/binder (*G/b*)	0.04	0.00	0.10	0.00	0.45	2.38
Fly ash/binder (*F/b*)	0.02	0.00	0.07	0.00	0.54	3.49

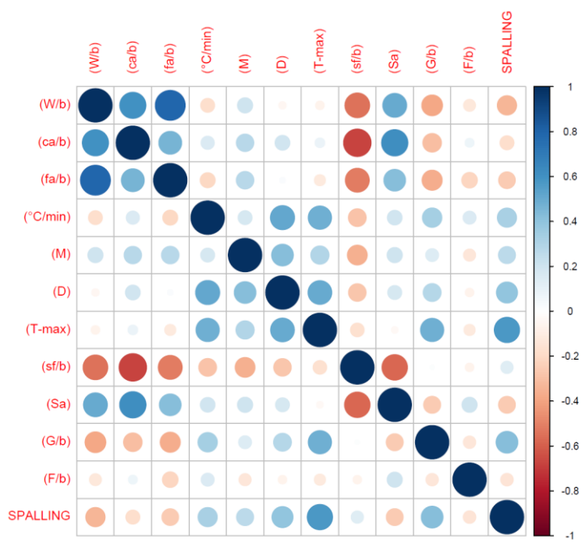

Pearson correlation

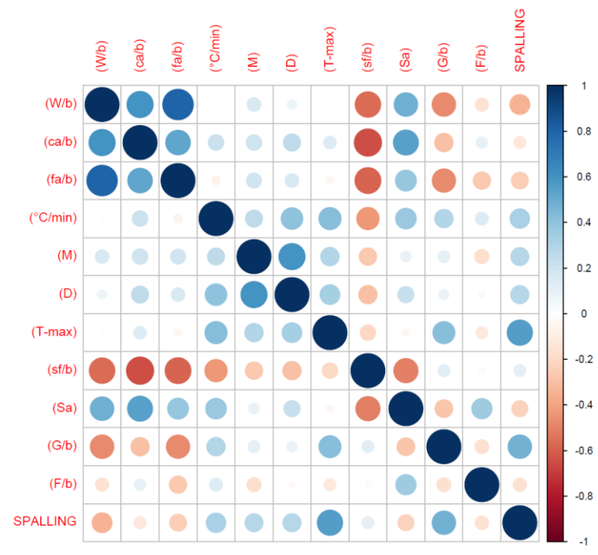

Spearman correlation

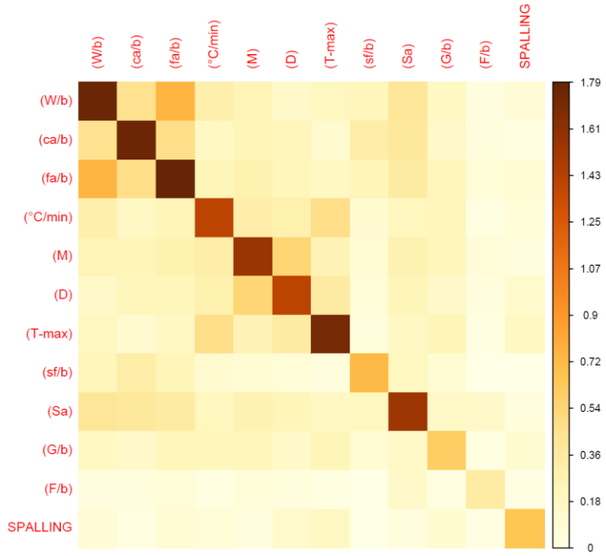

Mutual information

155

This is a preprint draft. The published article can be found at: https://doi.org/10.1007/s10694-022-01290-7.

Please cite this paper as:

Tapeh, A., Naser, M.Z. (2022). Discovering Graphical Heuristics on Fire-induced Spalling of Concrete through eXplainable Artificial Intelligence. *Fire Technology*. https://doi.org/10.1007/s10694-022-01290-7.

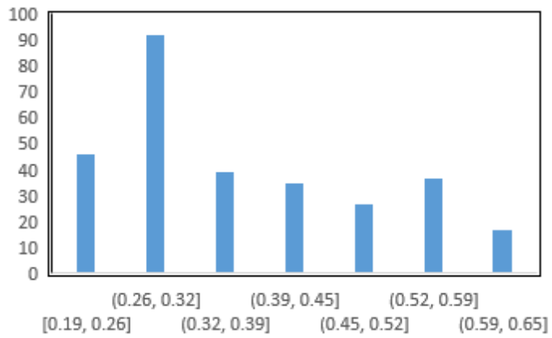

Water/binder (*W/b*)

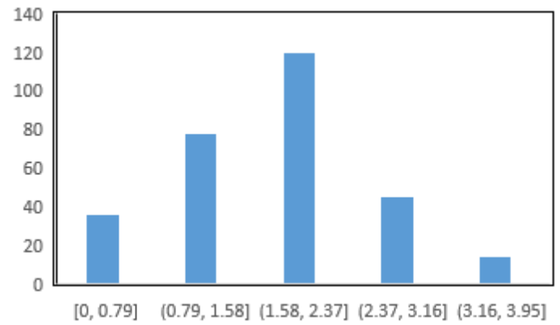

Coarse aggregate/binder (*Ca/b*)

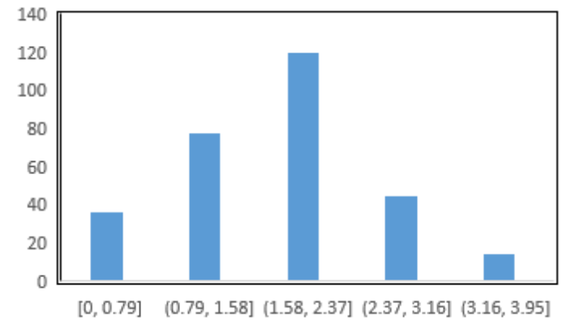

Fine aggregate/binder ratio (*Fa/b*)

Heating rate (*H*, °C/min)

Moisture content of concrete (*M*)

Characteristic distance of the concrete (*D*)

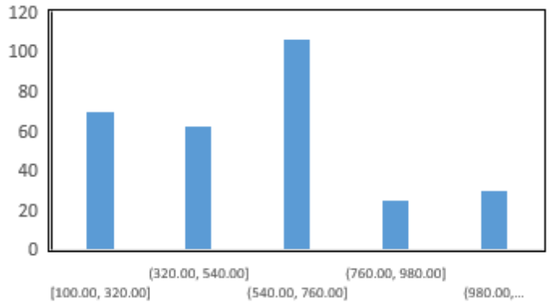

Maximum exposure temperature (T_{max}, °C)

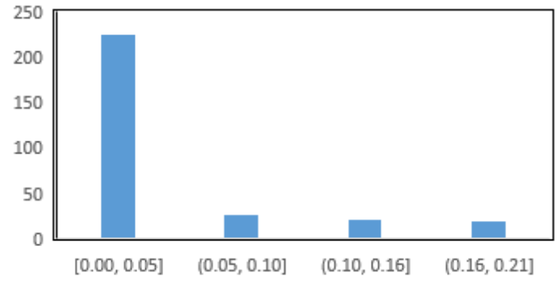

Silica fume/binder (*Sf/b*)

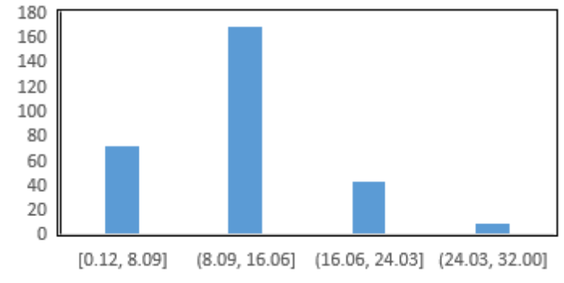

Maximum size of aggregate (*Sa*)

This is a preprint draft. The published article can be found at: https://doi.org/10.1007/s10694-022-01290-7.

Please cite this paper as:

Tapeh, A., Naser, M.Z. (2022). Discovering Graphical Heuristics on Fire-induced Spalling of Concrete through eXplainable Artificial Intelligence. *Fire Technology*. https://doi.org/10.1007/s10694-022-01290-7.

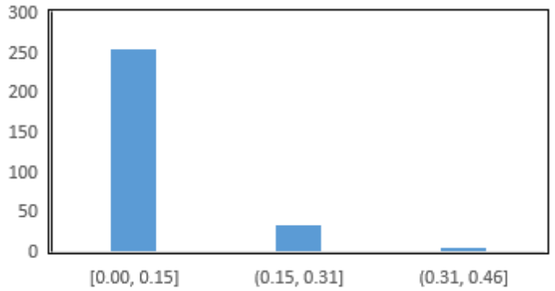

GGBS/binder (*G/b*)

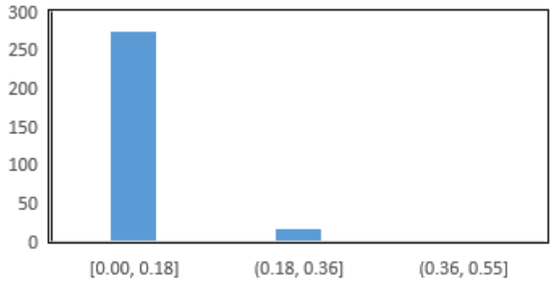

Fly ash/binder (*F/b*)

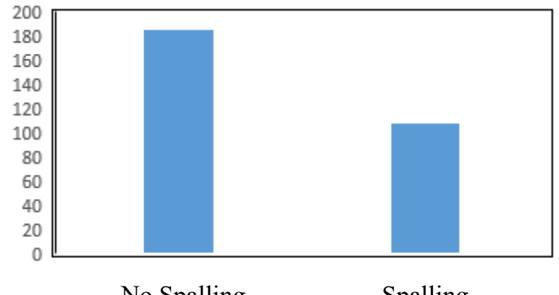

Fig. 1 Details of the compiled database

This is a preprint draft. The published article can be found at: https://doi.org/10.1007/s10694-022-01290-7.

Please cite this paper as:

Tapeh, A., Naser, M.Z. (2022). Discovering Graphical Heuristics on Fire-induced Spalling of Concrete through eXplainable Artificial Intelligence. *Fire Technology*. https://doi.org/10.1007/s10694-022-01290-7.

2.2 Details of Algorithms and Approach

This section outlines the proposed approach. First, we discuss the XAI algorithms used to arrive at graphical heuristics, and then we outline the procedure to develop AI-based nomograms.

2.2.1 XAI Algorithms and Methodology

Three algorithms are used herein. These include the XGBoost, Light Gradient Boosting Machine (LGBM), and Keras Slim Residual Neural Network (KSRNN). Each algorithm is briefly described herein as thorough discussions, and codes can be found in their original sources.

The XGboost is a tree-like algorithm that was first published by Chen and Guestrin [67] (and the code of the used XGBoost can be found online at [68,69]). This algorithm has a weighted quantile approximation function that determines split candidates in a tree and the sparsity-aware split finding. The XGboost uses a pre-sorted algorithm and a histogram-based algorithm for computing the best split. The devised algorithm was tweaked with the following settings: learning rate = 0.05, maximum tree depth = 3.0, minimum split loss = 0.01, subsample feature = 1.0, and number of estimators = 500.

The LGBM algorithm was developed and published by Microsoft [70]. This algorithm adopts two techniques, namely: gradient-based one-side sampling (to identify the most informative observations) and exclusive feature bundling (to group features in a near-lossless way). The LGBT algorithm can be found at [71] and tweaked herein with the following settings: learning rate = 0.01, maximum depth = "none", and the number of estimators = 500.

Keras is an open library for developing neural networks [72] and can be readily found at [73]. In a slim residual network, only one hidden layer exists with a direct connection linking data points to the outputs. In the used KSRNN, default settings of a learning rate of 0.01, along with a *Prelu* and *Sigmoid* as activation functions for the hidden and output layers, *Adam* optimizer, batch size = 5.0, and one hidden layer of 64 units were used.

Each of the above algorithms was applied individually to the compiled database to establish a comparative study. The training process for each algorithm begins with randomly shuffling and splitting the database into three sets[7] (T: training, V: validation, and S: testing, where the T set is the largest). Each algorithm is first trained on the T set, validated against the V set, and independently tested against the S set. In addition to the above procedure, a *k*-fold cross-validation procedure is also applied. In such a procedure, the T set is randomly split up into *k* groups, wherein the model is trained using *k*-1 sets and then validated on the last *k* set. This procedure is repeated *k* times until each unique set has been used as the validation set. *k* in this study was taken as 10.

During every stage, each algorithm is examined via performance metrics. Since this work explores the spalling phenomenon (as if a concrete mixture spalls or not), classification metrics will be

[7] For a fair comparison, these sets were kept identical when applied to each algorithm.

This is a preprint draft. The published article can be found at: https://doi.org/10.1007/s10694-022-01290-7.

Please cite this paper as:

Tapeh, A., Naser, M.Z. (2022). Discovering Graphical Heuristics on Fire-induced Spalling of Concrete through eXplainable Artificial Intelligence. *Fire Technology*. https://doi.org/10.1007/s10694-022-01290-7.

adopted. Given the unique derivation of metrics, these constructs often have advantages and disadvantages; thus, it is best to utilize a series of independent metrics [74]. Three metrics are used: Area under the ROC curve (AUC), Log Loss Error (LLE), and the confusion matrix. The former two metrics are listed in Table 2, and the latter describes a matrix that compares the number of correct predictions to those of the poorly predicted instances with values in the main diagonal depicting correct predictions.

Table 2 List of selected performance metrics.

Area under the ROC curve (AUC)	$AUC = \sum_{i=1}^{N-1} \frac{1}{2}(FP_{i+1} - FP_i)(TP_{i+1} - TP_i)$ *where, FP: number of false positives, TP: number of true positives.* *Note: values approaching unity imply high predictivity.*
Log Loss Error (LLE)	$LLE = -\sum_{c=1}^{M} A_i log P$ *where, M: number of classes, c: class label, y: binary indicator (0 or 1) if c is the correct classification for a given observation.* *Note: values approaching zero imply high predictivity. LLE penalizes for being confident in the wrong prediction.*
Confusion Matrix	$True\ Positive\ Rate\ (TPR) = Sensitivity = \frac{TP}{TP+FN}$ $True\ Negative\ Rate\ (TNR) = Specificity = \frac{TN}{TN+FP}$ $Accuracy\ (ACC) = \frac{TP+TN}{TP+TN+FP+FN}$ *where, TN: number of true negatives), FN: number of false negatives.*

A: actual measurements, *P*: predictions, *n*: number of data points.

In a confusion matrix, three main elements are of significance, namely; True Positive Rate (TPR) or Sensitivity, True Negative Rate (TNR) or Specificity, and Accuracy (ACC). The TPR and TNR metrics define the actual positive cases correctly identified (i.e., correctly predicting spalling for a mixture that has spalled in tests) and the actual negative cases correctly identified, respectively. On the other hand, the ACC presents a ratio of the correct predictions to the total number of samples, respectively. All the metrics formulas are described in Table 2 [74].

Once each algorithm is properly validated and tested, then explainability tools are augmented to arrive at insights into the spalling phenomenon. More specifically, the SHAP method [42] is first

This is a preprint draft. The published article can be found at: https://doi.org/10.1007/s10694-022-01290-7.

Please cite this paper as:

Tapeh, A., Naser, M.Z. (2022). Discovering Graphical Heuristics on Fire-induced Spalling of Concrete through eXplainable Artificial Intelligence. *Fire Technology*. https://doi.org/10.1007/s10694-022-01290-7.

applied to rank the importance of the used features (i.e., identify those features with the largest influence upon predictions from each model (e.g., identify the highly used features). Then, a partial dependence plot (PDP) is constructed for each XAI model. A PDP displays the marginal effect of an individual feature while holding other features constant on model predictions [43]. A more thorough discussion on the fundamentals of explainability measures can be found elsewhere [42,43] as well as in our recent work [37], which is tailored for engineering applications, and [35], which tackled the fire response of concrete columns.

2.2.2 Development of Nomogram

The selected procedure to develop a nomogram requires utilizing the logistic regression (LR) algorithm. LR, formulated by David Cox [75], is one of the most widely used supervised learning algorithms for binary classification problems. The LR algorithm primes the *Sigmoid* function. The used LR algorithm was trained and validated using the outlined procedure in the previous section. The *R* programming language (version 4.1.2) was heavily used to develop the proposed nomogram.

Once the LR algorithm is fully validated, the spalling occurrence is fitted through the following algebraic representation (Eq. 1). This representation denotes that the occurrence of spalling is calculated via the identified features of the compiled database. Then, the probability of spalling occurrence is calculated using a logistic, *Sigmoid*, equation (Eq. 2). Equation 2 returns values close to zero or unity if the examined concrete mixture is prone to spall, or not inclined to spall, respectively. More specifically, the *rms* (*regression modeling strategy*) *R* package [76] and the *sigmoid* function in the *R Toolbox* are used to develop the nomogram and arrive at the probability of spalling.

$$Spalling \sim W/b + Ca/b + Fa/b + H + M + D + T + Sf/b + Sa + G/b + F/b \quad \text{Eq. 1}$$

$$Propensity\ to\ Spalling = \frac{1}{1+exp^{-(\beta 0+\beta 1X1+\beta 2X2+\cdots)}} \quad \text{Eq. 2}$$

Where, β_0, β_1, etc., are coefficients[8] derived during the training process, and X_1, X_2, etc., are the features identified in our database (and those listed in Eq. 1). Both the developed nomogram and an example of how to properly apply this nomogram are provided in the following section and Appendix A. In addition, Appendix B and Appendix C outline the codes used to create the proposed nomogram and web application with a graphical user interface that does not require coding experience to operate, respectively.

[8]Spalling=-9.6005W/b+ 0.3444Ca/b+1.2066Fa/b+0.0089H+40.3826M+0.0224D+0.0070T+14.2181Sf/b-0.1055Sa+4.2498G/b+0.3490F/b-6.1001

This is a preprint draft. The published article can be found at: https://doi.org/10.1007/s10694-022-01290-7.

Please cite this paper as:

Tapeh, A., Naser, M.Z. (2022). Discovering Graphical Heuristics on Fire-induced Spalling of Concrete through eXplainable Artificial Intelligence. *Fire Technology*. https://doi.org/10.1007/s10694-022-01290-7.

3.0 Findings and Discussion

3.1 XAI Insights (heuristics)

We start our discussion by showcasing the results from the XAI analysis. First, we report the performance of the XAI models and then dive into the derived heuristics.

The performance of the XGboost, LGBM, and KSRNN is shown in Table 3 during the training, validation, and testing stages. As one can see, the three models have comparable performance, with the XGBoost being a clear favorite since it scores the highest in the majority of performance metrics listed in Table 3. These results, as obtained from different metrics, further our confidence in the developed models.

Table 3 Performance of the developed models for training/validation/testing regimes.

	XGboost			LGBM			KSRNN		
AUC	*0.994*	*0.968*	*0.967*	0.954	0.949	0.937	0.950	0.930	0.899
LLE	*0.108*	*0.255*	*0.271*	0.311	0.298	0.358	0.331	0.341	0.425
Sensitivity	*0.944*	*0.907*	*1.000*	0.944	0.779	0.818	0.889	0.837	0.955
Specificity	*1.000*	0.926	0.861	1.000	0.953	0.940	1.000	0.872	0.806
Accuracy	*0.978*	*0.919*	*0.914*	0.978	0.889	0.897	0.957	0.859	0.862

3.1.1 Feature Importance

The feature importance in each model was calculated using the SHAP method and is plotted for all features in Fig. 2. As one can see, the three models agree for the most part on the importance of the individual features (with some outliers such as *Sf/b* and *F/b* possibly due to the algorithmic nature of KSRNN). Furthermore, four features are noted to have the highest importance (i.e., ranging between 0.5-1.0) across all the algorithms. These include *T*, *W/b*, *H,* and *M* and seem to resemble the same features holistically identified by notable works and existing theories, thereby mirroring further confidence in the developed models [4,7]. The importance of features other than those identified above varies between minor and negligible.

This is a preprint draft. The published article can be found at: https://doi.org/10.1007/s10694-022-01290-7.

Please cite this paper as:

Tapeh, A., Naser, M.Z. (2022). Discovering Graphical Heuristics on Fire-induced Spalling of Concrete through eXplainable Artificial Intelligence. *Fire Technology*. https://doi.org/10.1007/s10694-022-01290-7.

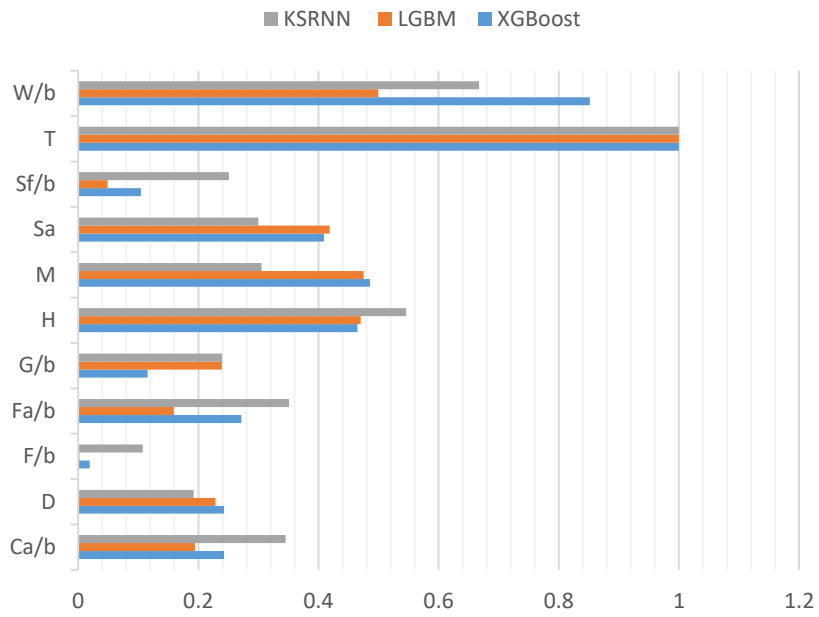

Fig. 2 Feature importance

3.1.2 Partial Dependence Plots (PDP)

Now that the importance of each feature has been established, it is time to develop partial dependence plots (PDP). Figure 3 depicts the PDP for each feature as generated by each of the three algorithms. A look into Fig. 3 shows that there is a convergence between all PDP; wherein general trends are mirrored well across the three models.

We keep our primary discussion to the aforenoted four features of the highest importance (i.e., *T*, *W/b*, *H,* and *M*). It is clear that higher temperatures are associated with a larger propensity to spalling. However, temperatures beyond 600ºC do not seem to affect the tendency to spall by much, wherein there is a high propensity to spalling (also agrees with [77–79]). When it comes to *W/b*, lower ratios (< 0.3) seem to have a high tendency to spalling. This may be evident in concretes of higher strength (HSC and UHPC) – also reported by [80]. However, the same PDP also shows that *W/b* of 0.45 can have higher spalling as well[9]. Similarly, higher values of *H*[10] (larger than 2.5ºC/min) and *M* (larger than 3%[11]) are associated with higher spalling frequency.

[9]This anomaly was also reported by [101].

[10]Noumowe et al. [82] and Klingsch [80] reported the possible occurrence of spalling at relatively low heating rates of 0.5°C/min. Hertz [14] also showed that "dense" concrete may spall at heating rate of 1°C/min.

[11]A similar observation was made by [14,86], and in fact, the recommended value of 3% is proposed by Eurocode 2 [87].

On another front, the maximum size of aggregate seems to have a distinct response to spalling (notably for smaller aggregate sizes[12]). Finally, features such as *F/b*, *Sf/B,* and *G/b* do not seem to adversely affect the spalling tendency of concrete mixtures[13].

When combined, the resulting PDP can be thought of as heuristics to identify if a specific concrete mixture is likely to spall or not under fire. These heuristics are shown at the bottom of Fig. 3 as devised from the three algorithms. The same heuristics show that concrete mixtures with relatively moderate *W/b* ratio and low *T*, *H,* and *M* are expected to be less prone to spalling than other mixtures.

[12]A similar observation was made by [51,84].

[13]For transparency, we speculate that a more comprehensive database to contain varying observations of these features (as shown in Fig. 1) alter change this finding. Thus, we are proponents of frequently updating the proposed solutions (on a rotating basis of 2-5 years).

This is a preprint draft. The published article can be found at: https://doi.org/10.1007/s10694-022-01290-7.

Please cite this paper as:

Tapeh, A., Naser, M.Z. (2022). Discovering Graphical Heuristics on Fire-induced Spalling of Concrete through eXplainable Artificial Intelligence. *Fire Technology*. https://doi.org/10.1007/s10694-022-01290-7.

281

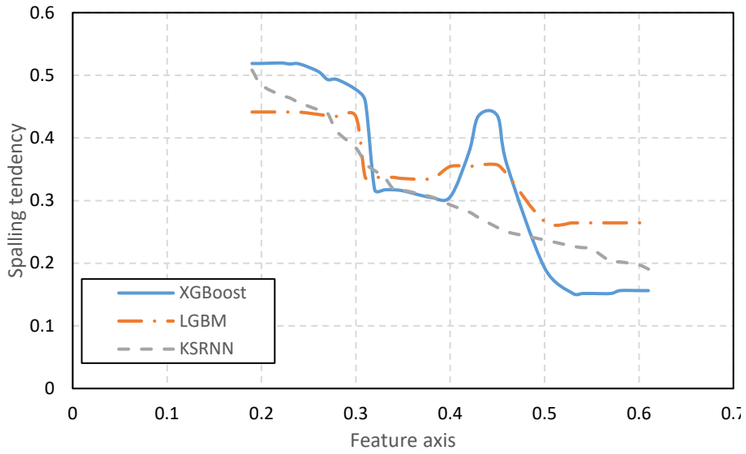

Water/binder (*W/b*)

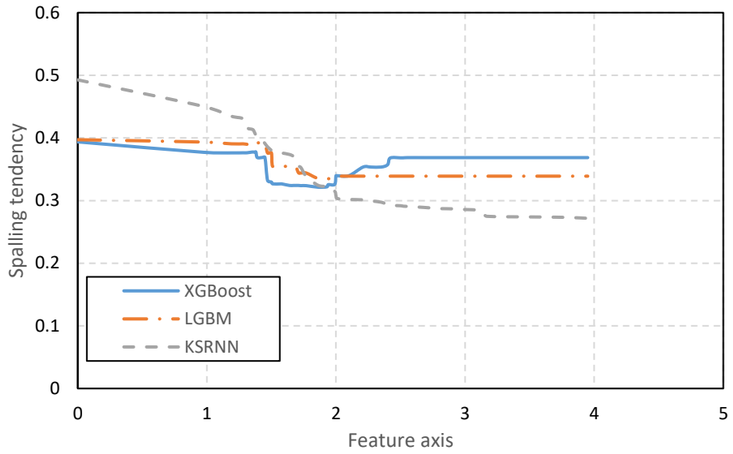

Coarse aggregate/binder (*Ca/b*)

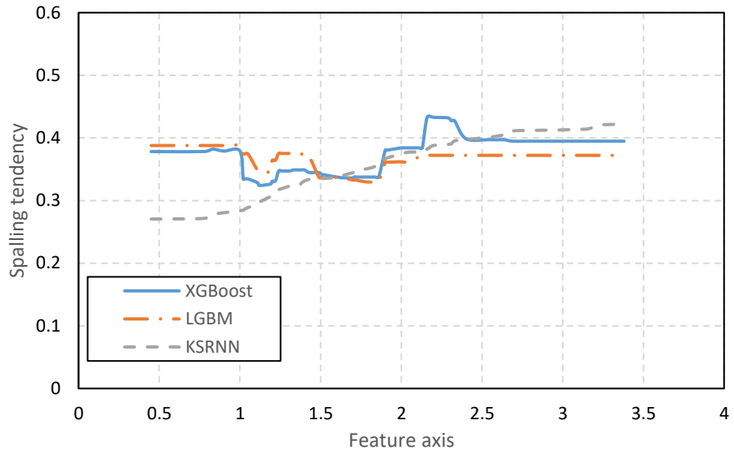

Fine aggregate/binder ratio (*Fa/b*)

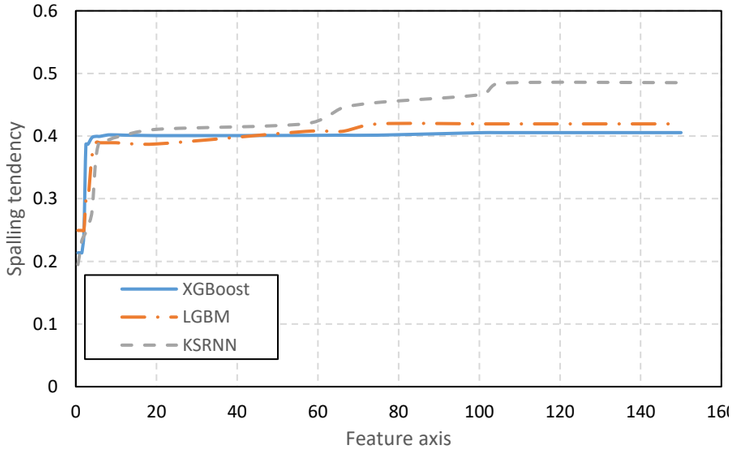

Heating rate (*H*, °C/min)

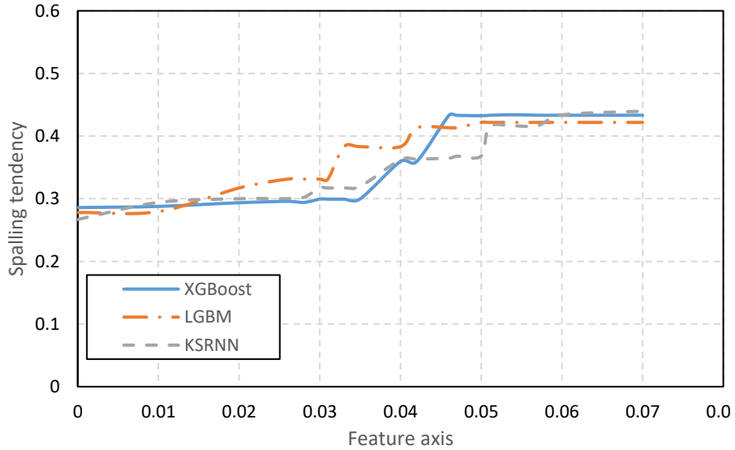

Moisture content of concrete (*M*)

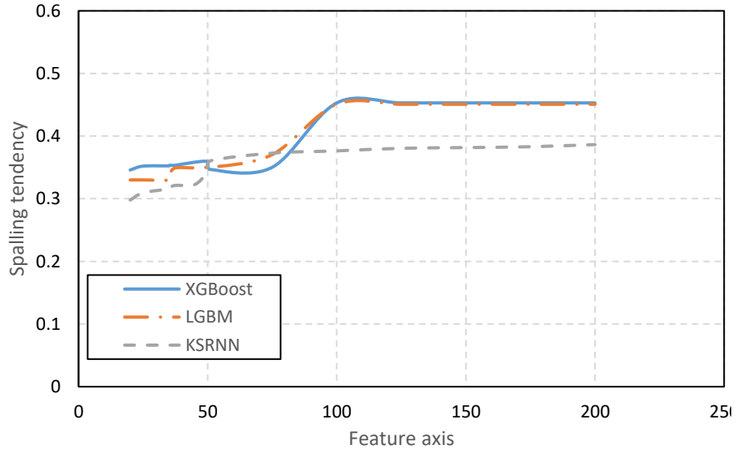

Characteristic distance (*D*)

This is a preprint draft. The published article can be found at: https://doi.org/10.1007/s10694-022-01290-7.

Please cite this paper as:

Tapeh, A., Naser, M.Z. (2022). Discovering Graphical Heuristics on Fire-induced Spalling of Concrete through eXplainable Artificial Intelligence. *Fire Technology*. https://doi.org/10.1007/s10694-022-01290-7.

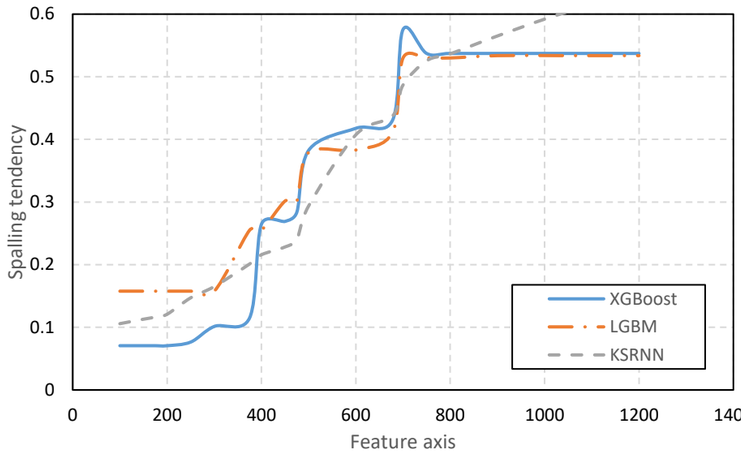

Maximum exposure temperature (T_{max}, °C)

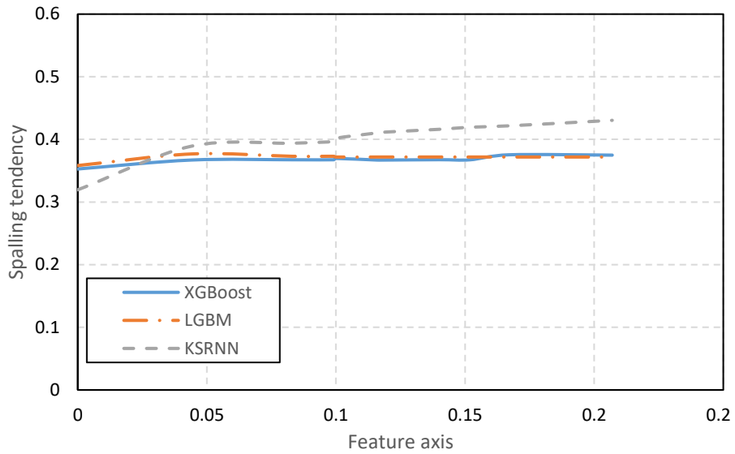

Silica fume/binder (*Sf/b*)

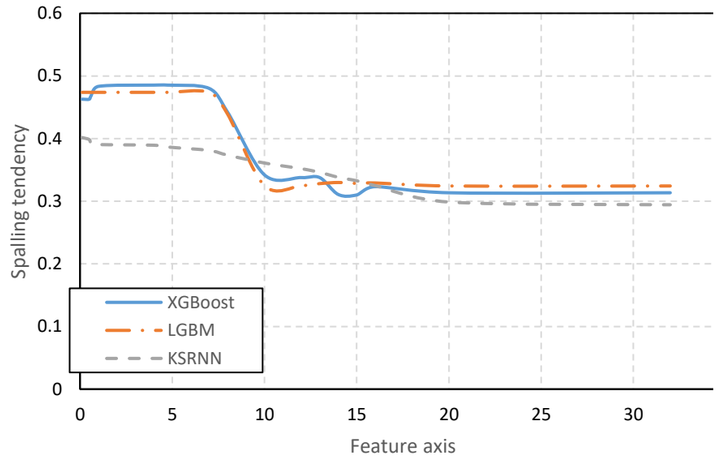

Maximum size of aggregate (*Sa*)

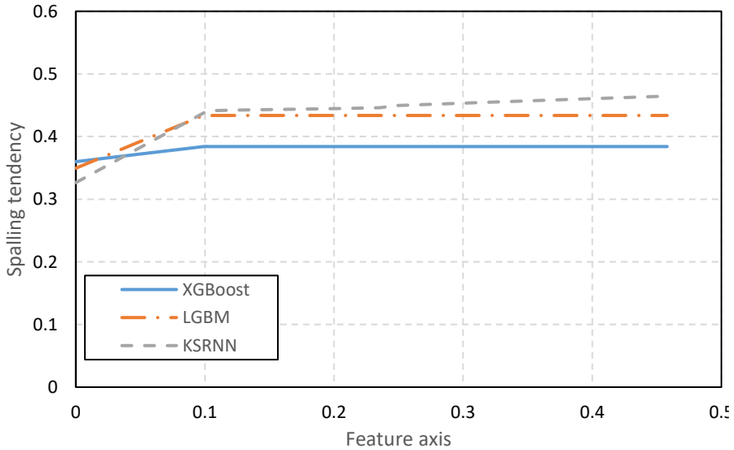

GGBS/binder (*G/b*)

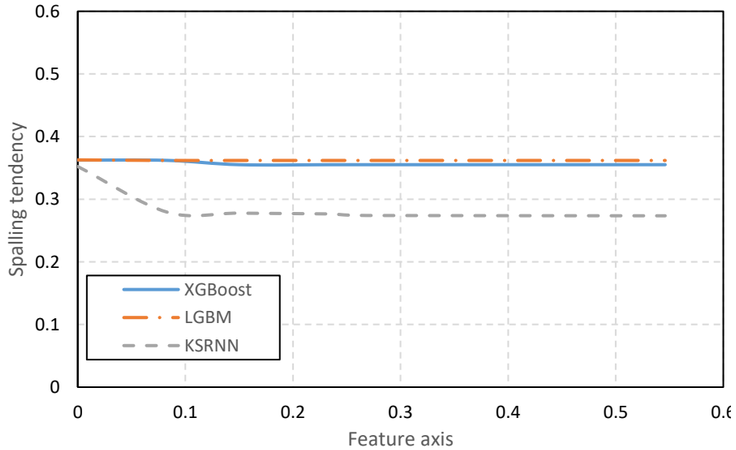

Fly ash/binder (*F/b*)

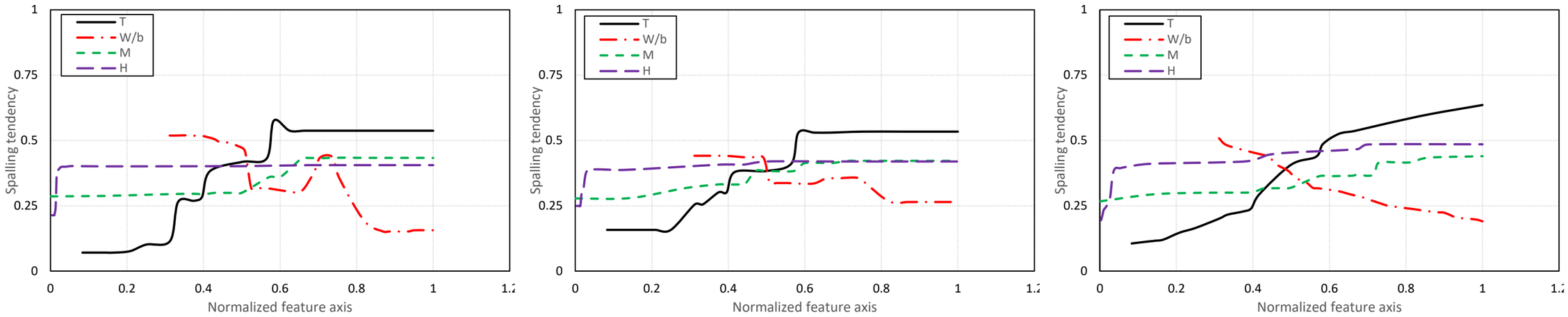

Combined DPD from XGBoost | Combined DPD from LGBM | Combined DPD from KSRNN

Fig. 3 Heuristics from the XAI insights [Note: The vertical axis represents the *spalling tendency* where zero implies less tendency to spalling unity implies a high tendency to spalling. For illustrative purposes, the vertical axis was capped at 0.6, except for the bottom three PDP]

3.2 Nomogram

Mirroring the previous section, we start by validating the LR model, which achieved an AUC of 92% and 100% in training and testing, respectively. In addition, the model achieved 0.910, 1.000, and 0.961 in sensitivity, specificity, accuracy, respectively. As one can see, the model has a favorable performance.

3.2.1 Development of Nomogram

The developed nomogram can be seen in Fig. 4 (displayed on the next page for legibility). This nomogram assigns the propensity of a given concrete mixture to spalling based on attaining a cumulative number of points (ranging from 0-100). This cumulative number of points is the arithmetic sum of the assigned points to each independent feature and is also used to estimate the probability of spalling. As one can see, given that each feature is scaled independently, the scale of the points pertaining to each feature must also be properly scaled. The nomogram shows that concrete mixtures with a total number of points ranging between 133-251 might experience spalling with a varying degree of certainty.

For example, when the total points for a given mixture is less than 133, this mixture is not vulnerable to spalling. On the other hand, when the total points for a given mixture is larger than 193, then the concrete mixture is more expected to be vulnerable to spalling. Mixtures with a total number of points exceeding 251 are highly vulnerable to spalling. Thus, the range between 133-193is a grey area where the expectation of spalling/no spalling of mixtures is heavily influenced by the combination of mixture proportions and heating conditions.

In addition, a companion to the nomogram is Table 4, which lists all the features and their corresponding scaled points. Thus, rather than finding points from the nomogram, a user may refer to Table 6 to assess if the desired concrete mixture will spall or not. For completion, the reader is to note that a dedicated solved example is provided in Appendix A. Figure 5 depicts the expected probability of spalling occurrence as obtained from the LR model for our database (all 293 data points – not to be confused with the total number of points calculated from the nomogram).

This is a preprint draft. The published article can be found at: https://doi.org/10.1007/s10694-022-01290-7.

Please cite this paper as:

Tapeh, A., Naser, M.Z. (2022). Discovering Graphical Heuristics on Fire-induced Spalling of Concrete through eXplainable Artificial Intelligence. *Fire Technology*. https://doi.org/10.1007/s10694-022-01290-7.

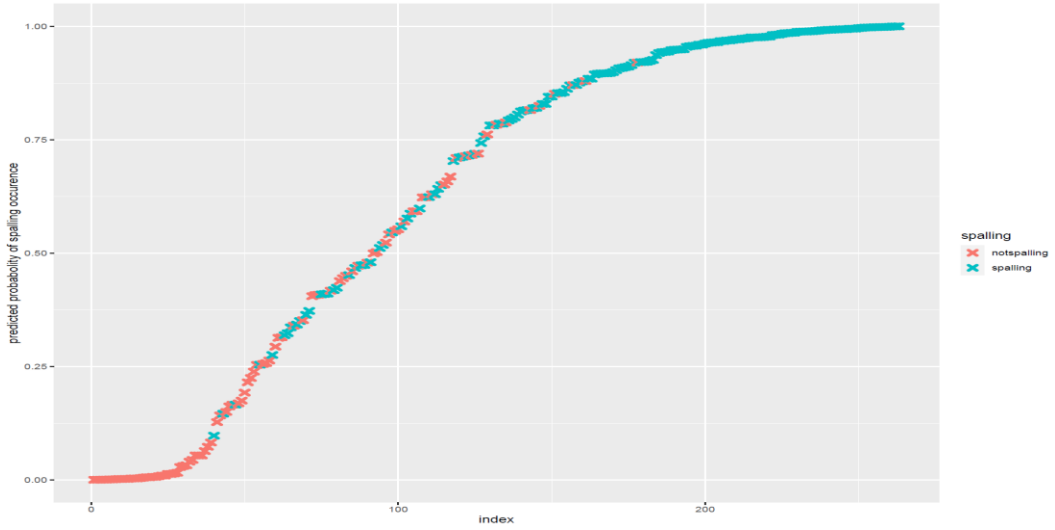

Fig. 5 Probability of spalling occurs per the LR model [Note: *Index* represents each of the observations listed in our database]

This is a preprint draft. The published article can be found at: https://doi.org/10.1007/s10694-022-01290-7.

Please cite this paper as:

Tapeh, A., Naser, M.Z. (2022). Discovering Graphical Heuristics on Fire-induced Spalling of Concrete through eXplainable Artificial Intelligence. *Fire Technology*. https://doi.org/10.1007/s10694-022-01290-7.

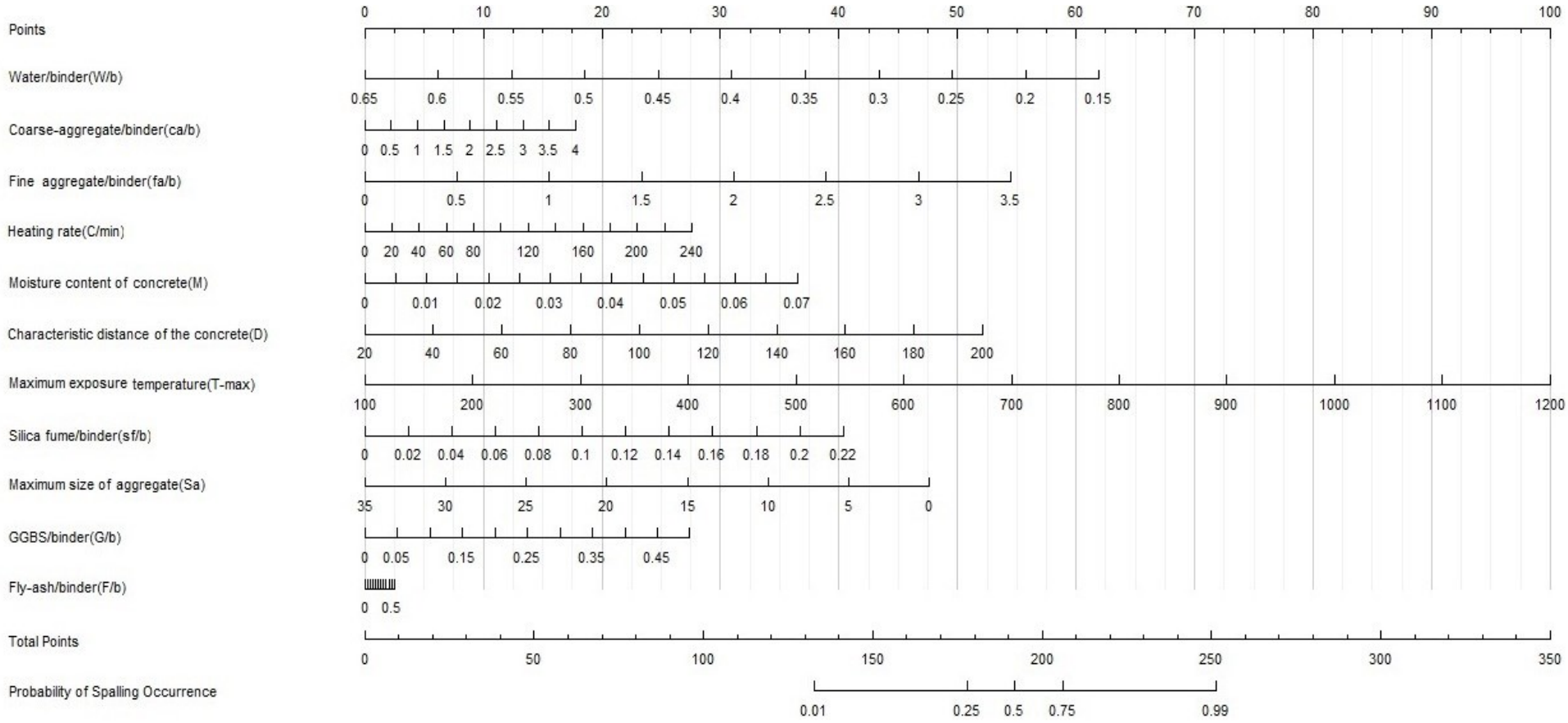

Fig. 4 The developed nomogram for predicting spalling in concrete mixtures

This is a preprint draft. The published article can be found at: https://doi.org/10.1007/s10694-022-01290-7.

Please cite this paper as:

Tapeh, A., Naser, M.Z. (2022). Discovering Graphical Heuristics on Fire-induced Spalling of Concrete through eXplainable Artificial Intelligence. *Fire Technology*. https://doi.org/10.1007/s10694-022-01290-7.

Table 5 Companion to the developed nomogram

Water-binder ratio	Points	Coarse aggregate/binder ratio	Points	Fine aggregate/binder ratio	Points	Heating rate	Points	Moisture content	Points	Characteristic distance of the concrete	Points	Maximum exposure temperature	points	Silica fume/binder ratio	Points	Maximum aggregate size	Points	GGBS/binder ratio	Points	Fly ash/binder ratio	Points	Total Points*	Probability of spalling occurrence
0.15	**62**	0.0	**0**	0.0	**0**	0	**1**	0.000	**0**	20	**0**	100	**0**	0.00	**0**	0	**48**	0.00	**0**	0.00	**0**	**133**	**0.01**
0.20	**56**	0.5	**2**	0.5	**8**	20	**2**	0.005	**3**	40	**6**	200	**9**	0.02	**4**	5	**41**	0.05	**3**	0.05	**0**	**178**	**0.25**
0.25	**50**	1.0	**4**	1.0	**16**	40	**5**	0.010	**5**	60	**12**	300	**18**	0.04	**7**	10	**34**	0.10	**5**	0.10	**0**	**192**	**0.50**
0.30	**43**	1.5	**7**	1.5	**23**	60	**7**	0.015	**8**	80	**17**	400	**27**	0.06	**11**	15	**27**	0.15	**8**	0.15	**1**	**206**	**0.75**
0.35	**37**	2.0	**9**	2.0	**31**	80	**9**	0.020	**10**	100	**23**	500	**36**	0.08	**15**	20	**20**	0.20	**11**	0.20	**1**	**251**	**0.99**
0.40	**31**	2.5	**11**	2.5	**39**	100	**11**	0.025	**13**	120	**29**	600	**45**	0.10	**18**	25	**14**	0.25	**14**	0.25	**1**		
0.45	**25**	3.0	**13**	3.0	**47**	120	**14**	0.030	**16**	140	**35**	700	**55**	0.12	**22**	30	**7**	0.30	**16**	0.30	**1**		
0.50	**19**	3.5	**16**	3.5	**54**	140	**16**	0.035	**18**	160	**41**	800	**64**	0.14	**26**	35	**0**	0.35	**19**	0.35	**2**		
0.55	**12**	4.0	**18**			160	**18**	0.040	**21**	180	**46**	900	**73**	0.16	**29**			0.40	**22**	0.40	**2**		
0.60	**6**					180	**21**	0.045	**23**	200	**52**	1000	**82**	0.18	**33**			0.45	**25**	0.45	**2**		
0.65	**0**					200	**23**	0.050	**26**			1100	**91**	0.20	**37**			0.50	**27**	0.50	**2**		
						220	**25**	0.055	**29**			1200	**100**	0.22	**40**					0.55	**2**		
						240	**28**	0.060	**31**														
								0.065	**34**														
								0.070	**36**														

*When the total points for a given mixture < 192 imply that spalling is not expected to take place, and when the total points for a given mixture > 206 imply that spalling is expected to occur.

This is a preprint draft. The published article can be found at: https://doi.org/10.1007/s10694-022-01290-7.

Please cite this paper as:

Tapeh, A., Naser, M.Z. (2022). Discovering Graphical Heuristics on Fire-induced Spalling of Concrete through eXplainable Artificial Intelligence. *Fire Technology*. https://doi.org/10.1007/s10694-022-01290-7.

4.0 Do Insights from XAI Match our Domain Knowledge on Fire-induced Spalling?

Recent, notable, and highly cited works on the fire-induced spalling front [3,10,14,80,81] converge on a few viewpoints: 1) the complexity of predicting spalling, 2) the discrepancy between existing theories, 3) inconsistency of reported results of tests, 4) poor/inexistence repeatability of published works and 5) the fact that concrete specimens of identical mixtures tested under identical conditions do not follow a consistent behavior (e.g., a specimen might spall where an identical specimen may not spall; thereby implying a highly random effect to accompany spalling). These facets further complicate our quest to unlock the spalling phenomenon and stretches the comfort zone of our pursuit to realizing deterministic solutions. The same facets are to be thought of as opportunities to motivate future works.

It is, then, not surprising that the reported insights from the carried out XAI analysis may echo some of the existing findings in our open literature and at the same time, may contradict others (as evident in the discussion and footnotes shown in Sec. 3.1.2) – specifically with regard to the influence of *W/b*, *T*, and *M,* as well as *H,* on spalling.

It is yet possible that our findings that match some of the cited works in this paper could be contrary to other published studies. For example, while Noumowe et al. [82], Klingsch [80] and Hertz [14] reported the occurrence of spalling at relatively low heating rates of 0.5-1.0°C/min (which deviates from our XAI findings that show the lower tendency to concrete to spall at such rates), others [80,83] have noted that spalling is unlikely to occur at such range. Similarly, our XAI analysis and [51,62,84] show that concretes with smaller aggregates are more vulnerable to spalling than those with larger aggregates, while [85] reports the opposite. On the moisture content, our analysis, as well as findings from [14,86], and Eurocode 2 [87], demonstrate that content of 3% leads to less propensity to spalling; others [50,88,89] have reported spalling for lower moisture content.

In other words, it is unlikely to find agreement between all sources on the influence of one particular parameter with regard to spalling. Rather, there seems to be a general consensus as to how a particular parameter influences spalling, and our heuristics and nomogram appear to capture this consensus.

We assume that the discrepancy between our analysis and that reported by other researchers could be due to differences between the concrete mixtures used in our database and those by the cited researchers (where exotic mixtures made of HSC and UHPC variants with unique fibers/admixtures were examined). In our database, the influence of steel or polypropylene fibers, as well as specifics of admixtures, presence of mechanical loading, and full heating history, were not considered. Building on the findings of [3,10,14,80], we believe that such features can influence model predictions to some extent. Thus, believe that a future study dedicated to exploring the combined influence of mixture proportions, mixture properties (i.e., compressive strength, etc.), size effect, and loading and heating conditions will shed more light on the spalling phenomenon.

This is a preprint draft. The published article can be found at: https://doi.org/10.1007/s10694-022-01290-7.

Please cite this paper as:

Tapeh, A., Naser, M.Z. (2022). Discovering Graphical Heuristics on Fire-induced Spalling of Concrete through eXplainable Artificial Intelligence. *Fire Technology*. https://doi.org/10.1007/s10694-022-01290-7.

Therefore, it is worth reminding our readers that the developed heuristics and nomograms are designed to show the *tendency* of concrete mixtures to spall, and these solutions are not to be thought of as deterministic tools. Keeping the latter in mind will solidify the position and applicability of the developed and to-be-developed heuristics and nomogram.

5.0 Conclusions

Fire-induced spalling is a complex problem. This paper presents an XAI approach (where AI algorithms were augmented with explainability measures) to create heuristics and nomograms to provide engineers and designers with tools to predict the occurrence of spalling in concrete mixtures. In order to develop the proposed tools, a series of fire tests collected from 293 real observations were compiled and analyzed. The outcome of the presented XAI analysis showcases the ease and potential of developing one-shot AI-based solutions to complex structural fire engineering problems. In addition, the following points can be inferred from this study:

- Insights from the XAI analysis seem to mirror our existing knowledge base and theories with regard to fire-induced spalling. It is then possible to use such insights to verify existing theories further and establish future research plans.
- Four parameters were shown to be of the highest importance with regard to spalling, namely, maximum achieved temperature, water/binder ratio, heating rate, and moisture content.
- Concrete mixtures with a combination of moderate water/binder ratio (of about 0.3), low heating rate (less than 2.5ºC/min), underwent high temperature (less than 500ºC), and have moisture content (less than 3%) are expected to be less prone to spalling.
- There is a need to fully and maximally leverage AI systems in our domain. The expected outcome from such utilization may accelerate finding solutions to ongoing and persistent problems.

Note

We invite interested users of the developed heuristics and nomograms to extend, test, and report their findings to realize improved versions of such tools.

Acknowledgment

The authors would like the acknowledge the following works of Dr. Liu's and Dr. Ye's [32–34,90,91] group, who managed to compile and share the database used herein. We encourage our readers to visit such works.

Conflict of Interest

The authors declare no conflict of interest.

References

[1] A.H. Buchanan, A.K. Abu, Fire Safety in Buildings, in: Struct. Des. Fire Saf., 2016.

389 doi:10.1002/9781118700402.ch2.

390 [2] V. Kodur, M. Naser, Structural Fire Engineering, 1st ed., McGraw Hill Professional,
391 2020.

392 [3] G.A. Khoury, Effect of fire on concrete and concrete structures, Prog. Struct. Eng. Mater.
393 2 (2000) 429–447. doi:10.1002/pse.51.

394 [4] J.-C.C. Liu, K.H. Tan, Y. Yao, A new perspective on nature of fire-induced spalling in
395 concrete, Constr. Build. Mater. 184 (2018) 581–590.
396 doi:10.1016/j.conbuildmat.2018.06.204.

397 [5] M.Z. Naser, Observational Analysis of Fire-Induced Spalling of Concrete through
398 Ensemble Machine Learning and Surrogate Modeling, J. Mater. Civ. Eng. 33 (2021).
399 doi:10.1061/(ASCE)MT.1943-5533.0003525.

400 [6] L.L.T. Phan, N.J.N. Carino, Effects of test conditions and mixture proportions on behavior
401 of high-strength concrete exposed to high temperatures, ACI Mater. (2002).
402 doi:10.14359/11317.

403 [7] V.K.R. Kodur, Innovative strategies for enhancing fire performance of high-strength
404 concrete structures, Adv. Struct. Eng. (2018). doi:10.1177/1369433218754335.

405 [8] G. Peng, X. Niu, K. Cheng, Research on Fire Resistance of Ultra-high-performance
406 Concrete: a Review, Cailiao Daobao/Materials Rev. (2017). doi:10.11896/j.issn.1005-
407 023X.2017.023.002.

408 [9] C. Kahanji, F. Ali, A. Nadjai, N. Alam, Effect of curing temperature on the behaviour of
409 UHPFRC at elevated temperatures, Constr. Build. Mater. 182 (2018) 670–681.
410 doi:10.1016/J.CONBUILDMAT.2018.06.163.

411 [10] V.K.R. Kodur, L. Phan, Critical factors governing the fire performance of high strength
412 concrete systems, Fire Saf. J. 42 (2007) 482–8. doi:10.1016/j.firesaf.2006.10.006.

413 [11] G.H.A.V. Der Heijden, L. Pel, O.C.G. Adan, Fire spalling of concrete, as studied by
414 NMR, Cem. Concr. Res. (2012). doi:10.1016/j.cemconres.2011.09.014.

415 [12] M.Z. Naser, Heuristic machine cognition to predict fire-induced spalling and fire
416 resistance of concrete structures, Autom. Constr. 106 (2019).
417 doi:10.1016/j.autcon.2019.102916.

418 [13] M.Z. Naser, Autonomous Fire Resistance Evaluation, ASCE Jounral Struct. Eng. 146
419 (2020). doi:10.1061/(ASCE)ST.1943-541X.0002641.

420 [14] K.D.D. Hertz, Limits of spalling of fire-exposed concrete, Fire Saf. J. 38 (2003) 103–116.
421 doi:10.1016/S0379-7112(02)00051-6.

422 [15] P. Kalifa, F. Menneteau, D. Quenard, Spalling and pore pressure in HPC at high
423 temperatures, Cem. Concr. Res. (2000). doi:https://doi.org/10.1016/S0008-

8846(00)00384-7.

[16] E.W.H. Klingsch, Explosive spalling of concrete in fire, Tese Doutorado. (2014). doi:10.3929/ethz-a-010076314.

[17] R. Jansson, Fire spalling of concrete - A historical overview, in: MATEC Web Conf., 2013. doi:10.1051/matecconf/20130601001.

[18] K.D. Hertz, L.S. Sørensen, Test method for spalling of fire exposed concrete, Fire Saf. J. (2005). doi:10.1016/j.firesaf.2005.04.001.

[19] M. Zeiml, D. Leithner, R. Lackner, H.A. Mang, How do polypropylene fibers improve the spalling behavior of in-situ concrete?, Cem. Concr. Res. (2006). doi:10.1016/j.cemconres.2005.12.018.

[20] Eurocode 2, 'Design of concrete structures"Part 1-2: General rules Structural fire design Euro code SS-EN-1992-1-2:2008, 3(July)., 2004.

[21] A. Committee, A.C. Institute, Building code requirements for structural concrete (ACI 318-08) and commentary, 2008.

[22] P. Kalifa, G. Chéné, C. Gallé, High-temperature behaviour of HPC with polypropylene fibres - From spalling to microstructure, Cem. Concr. Res. (2001). doi:10.1016/S0008-8846(01)00596-8.

[23] C.E. Majorana, V.A. Salomoni, G. Mazzucco, G.A. Khoury, An approach for modelling concrete spalling in finite strains, Math. Comput. Simul. (2010). doi:10.1016/j.matcom.2009.05.011.

[24] R. Jansson, L. Boström, The influence of pressure in the pore system on fire spalling of concrete, Fire Technol. (2010). doi:10.1007/s10694-009-0093-9.

[25] V.K.R. Kodur, Spalling in High Strength Concrete Exposed to Fire: Concerns, Causes, Critical Parameters and Cures, in: Adv. Technol. Struct. Eng., American Society of Civil Engineers, Reston, VA, 2000: pp. 1–9. doi:10.1061/40492(2000)180.

[26] L. Zhang, S.S. Hu, D.X. Chen, Z.Q. Yu, F. Liu, An experimental technique for spalling of concrete, Exp. Mech. (2009). doi:10.1007/s11340-008-9159-8.

[27] M.Z. Naser, Mechanistically Informed Machine Learning and Artificial Intelligence in Fire Engineering and Sciences, Fire Technol. (2021) 1–44. doi:10.1007/s10694-020-01069-8.

[28] M. Uysal, H. Tanyildizi, Estimation of compressive strength of self compacting concrete containing polypropylene fiber and mineral additives exposed to high temperature using artificial neural network, Constr. Build. Mater. (2012). doi:10.1016/j.conbuildmat.2011.07.028.

[29] A. Seitlllari, M.Z. Naser, Leveraging artificial intelligence to assess explosive spalling in

fire-exposed RC columns, Comput. Concr. (2019). doi:10.12989/cac.2019.24.3.271.

[30] M.Z. Naser, A. Seitllari, Concrete under fire: an assessment through intelligent pattern recognition, Eng. Comput. 36 (2020). doi:10.1007/s00366-019-00805-1.

[31] M.Z. Naser, V.K. Kodur, Explainable Machine Learning using Real, Synthetic and Augmented Fire Tests to Predict Fire Resistance and Spalling of RC Columns, (2021). https://arxiv.org/abs/2108.09862v1 (accessed September 18, 2021).

[32] J.-C. Liu, L. Huang, Z. Tian, H. Ye, Knowledge-enhanced data-driven models for quantifying the effectiveness of PP fibers in spalling prevention of ultra-high performance concrete, Constr. Build. Mater. 299 (2021) 123946. doi:10.1016/j.conbuildmat.2021.123946.

[33] J.C. Liu, Z. Zhang, Neural network models to predict explosive spalling of PP fiber reinforced concrete under heating, J. Build. Eng. (2020). doi:10.1016/j.jobe.2020.101472.

[34] J.C. Liu, Z. Zhang, A machine learning approach to predict explosive spalling of heated concrete, Arch. Civ. Mech. Eng. 20 (2020). doi:10.1007/s43452-020-00135-w.

[35] M.Z. Naser, V.K. Kodur, Explainable machine learning using real, synthetic and augmented fire tests to predict fire resistance and spalling of RC columns, Eng. Struct. 253 (2022) 113824. doi:10.1016/J.ENGSTRUCT.2021.113824.

[36] C. Rudin, Stop explaining black box machine learning models for high stakes decisions and use interpretable models instead, Nat. Mach. Intell. (2019). doi:10.1038/s42256-019-0048-x.

[37] M.Z. Naser, An engineer's guide to eXplainable Artificial Intelligence and Interpretable Machine Learning: Navigating causality, forced goodness, and the false perception of inference, Autom. Constr. 129 (2021) 103821. doi:10.1016/J.AUTCON.2021.103821.

[38] A. Doanvo, X. Qian, D. Ramjee, H. Piontkivska, A. Desai, M. Majumder, Machine Learning Maps Research Needs in COVID-19 Literature, Patterns. (2020). doi:10.1016/j.patter.2020.100123.

[39] H. Evesham, The History and Development of Nomography , CreateSpace Independent Publishing Platform, 2010.

[40] L. Hewes, H. Seward, The Design of Diagrams for Engineering Formulas and the Theory of Nomography, 1923. https://books.google.com/books?hl=en&lr=&id=jUMYAAAAIAAJ&oi=fnd&pg=PR9&dq=Nomography:+Theory+and+Application&ots=5iLCn1RXlS&sig=pNnqlunok2rBC_Atp7FgS9WGLFA (accessed January 24, 2022).

[41] E. Otto, Nomography, 2014. https://books.google.com/books?hl=en&lr=&id=oI_iBQAAQBAJ&oi=fnd&pg=PP1&dq=Nomography:+Theory+and+Application&ots=QU0huCiif3&sig=4yDjKb7Ye-

EWPkuQJTgtnVeTEGE (accessed January 24, 2022).

[42] S.M. Lundberg, S.I. Lee, A unified approach to interpreting model predictions, in: Adv. Neural Inf. Process. Syst., 2017.

[43] B.M. Greenwell, pdp: An R package for constructing partial dependence plots, R J. (2017). doi:10.32614/rj-2017-016.

[44] J.-. C. Liu, K.H. Tan, Mechanism of PVA fibers in mitigating explosive spalling of engineered cementitious composite at elevated temperature, Cem Concr Compos. 93 (2018). doi:10.1016/j.cemconcomp.2018.07.015.

[45] Li H. Experimental study on spalling behaviour and mechanical properties of reactive powder concrete after elevated temperature [Doctoral Thesis]: Harbin Institute of Technology; 2012., (n.d.).

[46] N. Yermak, P. Pliya, A.-L. Beaucour, A. Simon, A. Noumowé, Influence of steel and/or polypropylene fibres on the behaviour of concrete at high temperature: Spalling, transfer and mechanical properties, Constr. Build. Mater. 132 (2017) 240–250. doi:10.1016/j.conbuildmat.2016.11.120.

[47] L. Y, H. S-S, P. K, A. H, B. I., Mitigation of fire-induced spalling of concrete using recycled tyre polymer fibre, in: Proceedings of the 6th International Workshop on Concrete Spalling due to Fire Exposure, Sheffield, UK, n.d.

[48] Bosnjak J. Explosive spalling and permeability of high performance concrete under fire: numerical and experimental investigations [Doctor Thesis]: Universität Stuttgart 2014., (n.d.).

[49] G. Ruano, F. Isla, B. Luccioni, R. Zerbino, G. Giaccio, Steel fibers pull-out after exposure to high temperatures and its contribution to the residual mechanical behavior of high strength concrete, Constr Build Mater. 163 (2018). doi:10.1016/j.conbuildmat.2017.12.129.

[50] E. Klingsch, A. Frangi, M. Fontana, Explosive spalling of concrete in fire, IBK Bericht. 351 (2014). doi:10.3929/ETHZ-A-010076314.

[51] A. Mohd Ali, J. Sanjayan, M. Guerrieri, Specimens size, aggregate size, and aggregate type effect on spalling of concrete in fire, Fire Mater. 42 (2018). doi:10.1002/fam.2457.

[52] Hager I, Mróz K, Tracz T. Concrete propensity to fire spalling: Testing and observations. MATEC Web of Conferences; 2018: EDP Sciences. https://doi.org/10.1051/matecconf/201816302004, (n.d.).

[53] L.T. Phan, J.R. Lawson, F.L. Davis, Effects of elevated temperature exposure on heating characteristics, spalling, and residual properties of high performance concrete, Mater Struct. 34 (2001). doi:10.1007/BF02481556.

[54] L. Boström, U. Wickström, B. Adl-Zarrabi, Effect of specimen size and loading conditions on spalling of concrete, Fire Mater. 31 (2007). doi:10.1002/fam.931.

[55] M. Li, C. Qian, W. Sun, Mechanical properties of high-strength concrete after fire, Cem. Concr. Res. 34 (2004) 1001–1005. doi:10.1016/J.CEMCONRES.2003.11.007.

[56] R. Zhao, J.G. Sanjayan, Geopolymer and Portland cement concretes in simulated fire, Mag. Concr. Res. 63 (2011) 163–173. doi:10.1680/macr.9.00110.

[57] M.Z. Naser, V. Kodur, H.-T. Thai, R. Hawileh, J. Abdalla, V. V. Degtyarev, StructuresNet and FireNet: Benchmarking databases and machine learning algorithms in structural and fire engineering domains, J. Build. Eng. (2021) 102977. doi:10.1016/J.JOBE.2021.102977.

[58] R.B. Mugume, T. Horiguchi, Prediction of spalling in fibre-reinforced high strength concrete at elevated temperatures, Mater. Struct. 47 (2014) 591–604. doi:10.1617/s11527-013-0082-9.

[59] J.C. Liu, Z. Zhang, A machine learning approach to predict explosive spalling of heated concrete, Arch. Civ. Mech. Eng. (2020). doi:10.1007/s43452-020-00135-w.

[60] M.R. Bangi, T. Horiguchi, Pore pressure development in hybrid fibre-reinforced high strength concrete at elevated temperatures, Cem. Concr. Res. 41 (2011) 1150–1156. doi:10.1016/j.cemconres.2011.07.001.

[61] B. Zhang, Effects of moisture evaporation (weight loss) on fracture properties of high performance concrete subjected to high temperatures, Fire Saf. J. 46 (2011) 543–549. doi:10.1016/j.firesaf.2011.07.010.

[62] Z. Pan, J.G. Sanjayan, D.L.Y. Kong, Effect of aggregate size on spalling of geopolymer and Portland cement concretes subjected to elevated temperatures, Constr. Build. Mater. 36 (2012) 365–372. doi:10.1016/j.conbuildmat.2012.04.120.

[63] O. Arioz, Effects of elevated temperatures on properties of concrete, Fire Saf. J. (2007). doi:10.1016/j.firesaf.2007.01.003.

[64] K. Sideris, P. Manita, E. Chaniotakis, Performance of thermally damaged fibre reinforced concretes, Constr Build Mater. 23 (2009). doi:10.1016/j.conbuildmat.2008.08.009.

[65] B. Chen, J. Liu, Residual strength of hybrid-fiber-reinforced high-strength concrete after exposure to high temperatures, Cem Concr Res. 34 (2004). doi:10.1016/j.cemconres.2003.11.010.

[66] K.K. Sideris, Mechanical characteristics of self-consolidating concretes exposed to elevated temperatures, J Mater Civ. Eng. 19 (2007). doi:10.1061/(ASCE)0899-1561(2007)19:8(648).

[67] T. Chen, C. Guestrin, XGBoost: A scalable tree boosting system, in: Proc. ACM SIGKDD

Int. Conf. Knowl. Discov. Data Min., 2016. doi:10.1145/2939672.2939785.

[68] Scikit, sklearn.ensemble.GradientBoostingRegressor — scikit-learn 0.24.1 documentation, (2020). https://scikit-learn.org/stable/modules/generated/sklearn.ensemble.GradientBoostingRegressor.html (accessed February 9, 2021).

[69] XGBoost Python Package, Python Package Introduction — xgboost 1.4.0-SNAPSHOT documentation, (2020). https://xgboost.readthedocs.io/en/latest/python/python_intro.html#early-stopping (accessed February 10, 2021).

[70] G. Ke, Q. Meng, T. Finley, T. Wang, W. Chen, W. Ma, Q. Ye, T.Y. Liu, LightGBM: A highly efficient gradient boosting decision tree, in: Adv. Neural Inf. Process. Syst., 2017.

[71] LightGBM, Welcome to LightGBM's documentation! — LightGBM 3.1.1.99 documentation, (2020). https://lightgbm.readthedocs.io/en/latest/ (accessed February 9, 2021).

[72] H. Li, Z. Xu, G. Taylor, C. Studer, T. Goldstein, Visualizing the loss landscape of neural nets, in: Adv. Neural Inf. Process. Syst., 2018.

[73] Keras, GitHub - keras-team/keras: Deep Learning for humans, (2020). https://github.com/keras-team/keras (accessed February 9, 2021).

[74] M.Z. Naser, A.H. Alavi, Error Metrics and Performance Fitness Indicators for Artificial Intelligence and Machine Learning in Engineering and Sciences, Archit. Struct. Constr. 1 (2021) 3. doi:10.1007/s44150-021-00015-8.

[75] D.R. Cox, The Regression Analysis of Binary Sequences, J. R. Stat. Soc. Ser. B. (1959). doi:10.1111/j.2517-6161.1959.tb00334.x.

[76] CRAN - Package rms, (n.d.). https://cran.r-project.org/web/packages/rms/index.html (accessed January 27, 2022).

[77] J. Xiao, M. Xie, C. Zhang, Residual compressive behaviour of pre-heated high-performance concrete with blast-furnace-slag, Fire Saf. J. (2006). doi:10.1016/j.firesaf.2005.11.001.

[78] O. Arioz, Retained properties of concrete exposed to high temperatures: Size effect, Fire Mater. (2009). doi:10.1002/fam.996.

[79] Z. Xing, A.L. Beaucour, R. Hebert, A. Noumowe, B. Ledesert, Influence of the nature of aggregates on the behaviour of concrete subjected to elevated temperature, Cem. Concr. Res. (2011). doi:10.1016/j.cemconres.2011.01.005.

[80] E.W. Klingsch, Explosive spalling of concrete in fire, IBK-Bericht. (2014). doi:https://doi.org/10.3929/ethz-a-010076314.

[81] Y. Li, E.H. Yang, A. Zhou, T. Liu, Pore pressure build-up and explosive spalling in concrete at elevated temperature: A review, Constr. Build. Mater. (2021). doi:10.1016/j.conbuildmat.2021.122818.

[82] A. Noumowé, H. Carré, A. Daoud, H. Toutanji, High-Strength Self-Compacting Concrete Exposed to Fire Test, J. Mater. Civ. Eng. 18 (2006) 754–758. doi:10.1061/(ASCE)0899-1561(2006)18:6(754).

[83] P.J.E. Sullivan, The effect of temperature on concrete., in: Dev. Concr. Technol., Applied Science Publisher, 1979: pp. 1–50.

[84] A.Z. Mohd Ali, J. Sanjayan, M. Guerrieri, Effect of Aggregate Size on the Spalling of High-Strength Wall Panels Exposed to Hydrocarbon Fire, J. Mater. Civ. Eng. (2017). doi:10.1061/(asce)mt.1943-5533.0002087.

[85] R. Jansson, L. Boström, Experimental study of the influence of polypropylene fibres on material propertiesand fire spalling of concrete, in: Ire Des. Concr. Struct. – From Mater. Model. to Struct. Perform., 2007. https://www.diva-portal.org/smash/record.jsf?pid=diva2:647354 (accessed January 28, 2022).

[86] V.V. Zhukov, Explosive failure of concrete during a fire, 1975. https://scholar.google.com/scholar?hl=en&as_sdt=0%2C41&q=Zhukov%2C+V.V.%2C+Explosive+failure+of+concrete+during+a+fire&btnG= (accessed January 27, 2022).

[87] BSI, European Committee for Standardization, Design of concrete structures - Part 1-2: General rules - Structural fire design, 2004. doi:10.1002/jcp.25002.

[88] W.Z. Zheng, X.M. Hou, D.S. Shi, M.X. Xu, Experimental study on concrete spalling in prestressed slabs subjected to fire, Fire Saf. J. (2010). doi:10.1016/j.firesaf.2010.06.001.

[89] R. Jansson, L. Boström, Factors influencing fire spalling of self compacting concrete, Mater. Struct. Constr. (2013). doi:10.1617/s11527-012-0007-z.

[90] J.C. Liu, L. Huang, Z. Chen, H. Ye, A comparative study of artificial intelligent methods for explosive spalling diagnosis of hybrid fiber-reinforced ultra-high-performance concrete, Int. J. Civ. Eng. (2021). doi:10.1007/s40999-021-00689-7.

[91] J.C. Liu, Z. Zhang, Prediction of explosive spalling of heated steel fiber reinforced concrete using artificial neural networks, J. Adv. Concr. Technol. (2020). doi:10.3151/jact.18.227.

[92] M.Z. Naser, Demystifying Ten Big Ideas and Rules Every Fire Scientist & Engineer Should Know About Blackbox, Whitebox & Causal Artificial Intelligence, (2021). https://arxiv.org/abs/2111.13756v1 (accessed January 26, 2022).

[93] AISC, American Institute of Steel Construction, United States Am. (2017).

[94] A. Iasonos, D. Schrag, G. V. Raj, K.S. Panageas, How to build and interpret a nomogram

635 for cancer prognosis, J. Clin. Oncol. (2008). doi:10.1200/JCO.2007.12.9791.

636 [95] D.T. Zhang, D.H. Zhou, Nomograms for Determination of Effective Length of the
637 Unregular Frames Based on Mechanics and Steel Structure, Adv. Mater. Res. 886 (2014)
638 402–407. doi:10.4028/www.scientific.net/AMR.886.402.

639 [96] T. Chanmalai, B. Chang, K. Misaro, S. Hagos, T.B. Hanumanthareddy, Development of a
640 nomogram to predict the contact stress between an I-girder and a support roller, Eng. Solid
641 Mech. 9 (2021) 377–390. doi:10.5267/j.esm.2021.7.001.

642 [97] E. Alotaibi, O. Mostafa, N. Nassif, M. Omar, M.G. Arab, Prediction of Punching Shear
643 Capacity for Fiber-Reinforced Concrete Slabs Using Neuro-Nomographs Constructed by
644 Machine Learning, J. Struct. Eng. 147 (2021). doi:10.1061/(asce)st.1943-541x.0003041.

645 [98] X. Liu, Y. Han, C. Yu, F. Xiong, X. Zhou, Z. Deng, Reliability assessment on stability of
646 tunnel-type anchorages, Comput. Geotech. 125 (2020) 103661.
647 doi:10.1016/j.compgeo.2020.103661.

648 [99] M. Omar, A. Shanableh, A. Basma, S. Barakat, Compaction characteristics of granular
649 soils in United Arab Emirates, Geotech. Geol. Eng. 21 (2003) 283–295.
650 doi:10.1023/A:1024927719730.

651 [100] F.J. Colomer Mendoza, A. Ferrer Gisbert, A. Gallardo Izquierdo, M.D. Bovea, Safety
652 factor nomograms for homogeneous earth dams less than ten meters high, Eng. Geol. 105
653 (2009) 231–238. doi:10.1016/j.enggeo.2009.01.001.

654 [101] P.J.E. Sullivan, A probabilistic method of testing for the assessment of deterioration and
655 explosive spalling of high strength concrete beams in flexure at high temperature, Cem.
656 Concr. Compos. (2004). doi:10.1016/S0958-9465(03)00088-X.

657

This is a preprint draft. The published article can be found at: https://doi.org/10.1007/s10694-022-01290-7.

Please cite this paper as:

Tapeh, A., Naser, M.Z. (2022). Discovering Graphical Heuristics on Fire-induced Spalling of Concrete through eXplainable Artificial Intelligence. *Fire Technology*. https://doi.org/10.1007/s10694-022-01290-7.

Appendix A

This Appendix demonstrates an example for applying the developed nomogram. In this example, a concrete mixture tested by Ali et al. [51] and suffered from spalling was selected for analysis. The concrete mixture has the following features:

- Water/binder ratio = 0.27
- Coarse aggregate/binder ratio = 2.0
- Fine aggregate/binder ratio = 1.049
- Heating rate (°C/min) = 101
- Moisture content = 0.049
- Characteristic length of specimen (mm) = 100
- Maximum exposure temperature (°C) = 1034
- Silica fume/binder ratio = 0.0
- Maximum aggregate size (mm) = 7.0
- GGBS/binder ratio = 0.25
- Fly ash/binder ratio = 0.0

Using Nomogram:

In this example, the cumulative score for all 11 features is equal to 267. By depicting on the probability axes, the rate is close to 0.995% (which is very close to unity and hence indicates that spalling occurs for the concrete mixture).

Using Table: The same answer could have been arrived at through the supplementary table.

Total points = 48+9+17+11+25+23+86+0+39+14+0 = 272 points > 0.999 which is << Unity → Spalling is expected. [Note: underlined values were interpolated].

This is a preprint draft. The published article can be found at: https://doi.org/10.1007/s10694-022-01290-7.

Please cite this paper as:

Tapeh, A., Naser, M.Z. (2022). Discovering Graphical Heuristics on Fire-induced Spalling of Concrete through eXplainable Artificial Intelligence. *Fire Technology*. https://doi.org/10.1007/s10694-022-01290-7.

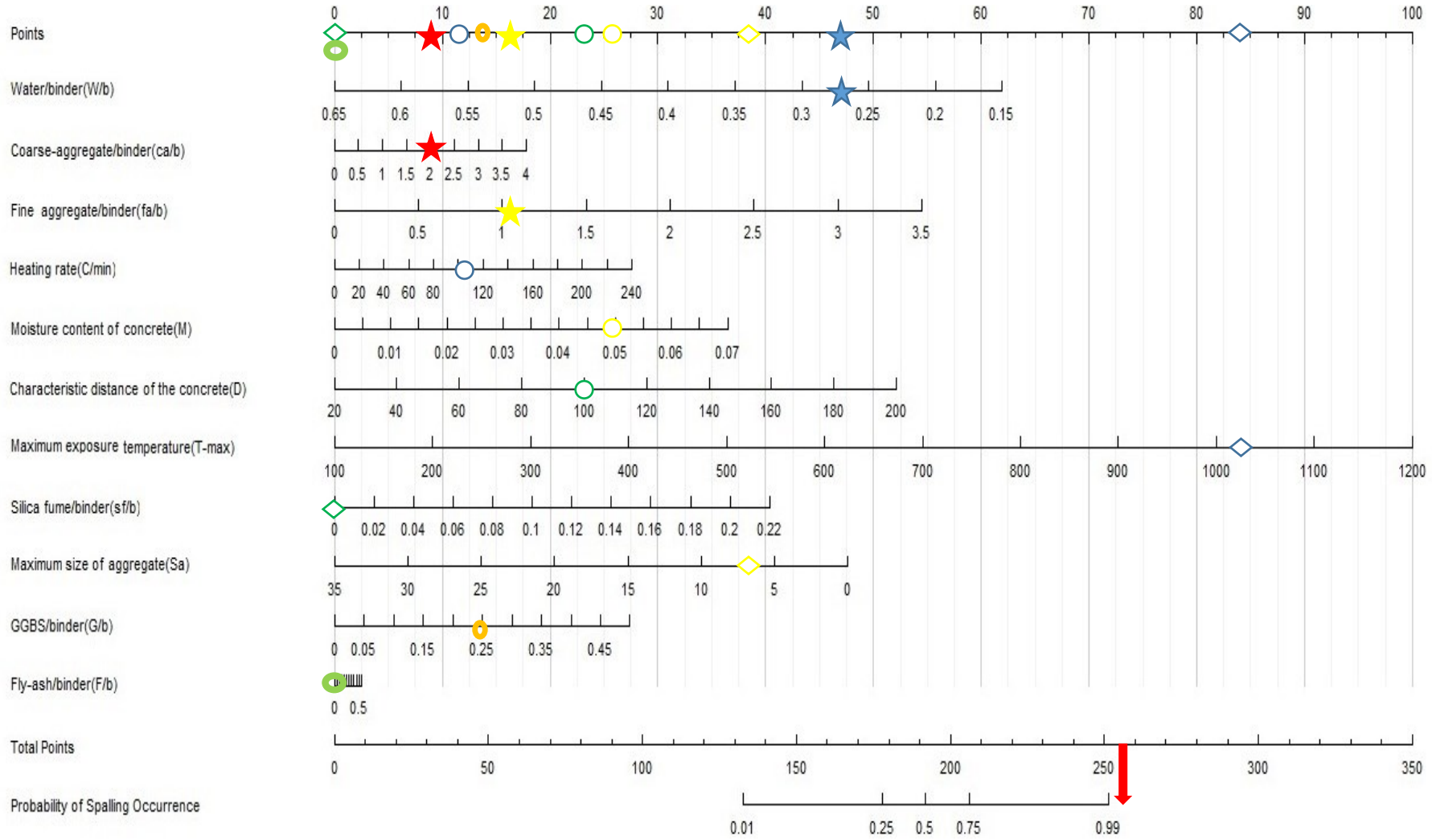

680

This is a preprint draft. The published article can be found at: https://doi.org/10.1007/s10694-022-01290-7.

Please cite this paper as:

Tapeh, A., Naser, M.Z. (2022). Discovering Graphical Heuristics on Fire-induced Spalling of Concrete through eXplainable Artificial Intelligence. *Fire Technology*. https://doi.org/10.1007/s10694-022-01290-7.

Water-binder ratio	Points	Coarse aggregate/binder ratio	Points	Fine aggregate/binder ratio	Points	Heating rate	Points	Moisture content	Points	Characteristic distance of the concrete	Points	Maximum exposure temperature	points	Silica fume/binder ratio	Points	Maximum aggregate size	Points	GGBS/binder ratio	Points	Fly ash/binder ratio	Points	Total Points	Probability of spalling occurrence
0.25 0.30 681	**50** **43**	2.0	**9**	1.5 1.0	**23** 16	100 101	**11** 11.01	0.05 0	**25**	100	**23**	1000	**86**	0.00	**0**	5 10	**41** **34**	0.2 50	**14**	0.00	**0**	251 272	0.99 <0.99

This is a preprint draft. The published article can be found at: https://doi.org/10.1007/s10694-022-01290-7.

Please cite this paper as:

Tapeh, A., Naser, M.Z. (2022). Discovering Graphical Heuristics on Fire-induced Spalling of Concrete through eXplainable Artificial Intelligence. *Fire Technology*. https://doi.org/10.1007/s10694-022-01290-7.

Appendix B

This appendix outlines our procedure for developing monograms.

The strategy for developing the proposed nomogram is enabled and adapted from the *R*-documentation. Our database includes 293 different samples and 11 distinct features imported via the *read.csv () function*. Then, each feature is titled, and the dependent variable (i.e., outcome titled, SPALLING is converted into binary values (i.e., 0 and 1 for "not spalling" and "spalling"), respectively)).

***R* code:**

```
> data=read.csv ('C: spalling.csv)
>colnames(data)<-C('Water/binder(W/b)','Coarse-aggregate/binder(ca/b)',
'Fine aggregate/binder(fa/b)','Heating rate(°C/min)','moisture content of
concrete(M)','Characteristic
Distance of the concrete(D)','maximum exposure temperature(T-max)','silica
fume/binder(sf/b)','maximum size of
aggregate(Sa)','GGBS/binder(G/b)','Flyash/binder(F/b)','SPALLING')
>data [data$SPALLING==0,] $SPALLING<-"notspalling"
>data [data$SPALLING==1,] $SPALLING<-"spalling"
>data$SPALLING<-as.factor (data$SPALLING)
```

Data partitioning is essential before developing and fitting ML models (in this instance, our logistic model). The binary outcome of the database (spalling and no spalling) was firstly separated from one another and the required portion of them (say, 70%, 80%, and 90% for the training set and corresponding 30%, 20%, and 10% for the testing set) created by the combination of the two first sections.

***R* code:**

```
> N<-nrow (data)
 data<-data[sample(1:N),]
 data.spalling <- subset(data, SPALLING=='spalling')
 data.notspalling <- subset(data, SPALLING=='notspalling')
 data.spalling.train <-data.spalling[seq(nrow(data.spalling)*9/10),]
 data.spalling.test <-data.spalling[(-seq(nrow(data.spalling)*9/10)),]
 data.notspalling.train <-data.notspalling[seq(nrow(data.notspalling)*9/10),]
 data.notspalling.test <-data.notspalling[(-seq(nrow(data.notspalling)*9/10)),]
 train.set <- rbind (data.spalling.train,data.notspalling.train)
 test.set <- rbind (data.spalling.test,data.notspalling.test)
```

Now is the time to use the packages that encompass the required functions for fitting the regression model to develop the nomogram. The *rms* package is deployed to fit the regression into the dataset and draw the nomogram. In essence, we start by defining *datadist ()* function to save the summary of predictor variable distribution. The aforenoted summaries in the *datadist ()* function include

This is a preprint draft. The published article can be found at: https://doi.org/10.1007/s10694-022-01290-7.

Please cite this paper as:

Tapeh, A., Naser, M.Z. (2022). Discovering Graphical Heuristics on Fire-induced Spalling of Concrete through eXplainable Artificial Intelligence. *Fire Technology*. https://doi.org/10.1007/s10694-022-01290-7.

data statistics such as plotting range, values to adjust to, and entire ranges of the predictor variable. Then, the *option ()* function reduces additional action to achieve any fitting information from source data. The logistic regression fitting is performed by *lrm ()* function. The *Nomogram ()* function converts the fitted logistic regression model *lrm ()* into a nomogram. The logistic model in this study is "*model.train.lrm*," and the nomogram model is "*nom.*"

***R* code:**

```
> model.lrm.train<-lrm (SPALLING ~. , train.set)
The first parameter in lrm () function shows that regression fitting is based on all
independent variable in the problem (here 11 distinct variable).
nom<-nomogram(model.lrm.train,fun=function(x)1/(1+exp(-x)),lp=FALSE,
fun.at=c(0.001,.01,.05,seq(.3,.9,by=.8),.95,.99,.999),
funlabel="Probability of spalling occurrence"
```

After fitting the regression model, the *fun ()* function, which is the sigmoid function, turns the linear regression into a logistic one. Also, the predicting axes in the nomogram can be scaled to accommodate different feature scales and probability range (taken as 0.001 to 0.999) using the *fun.at ()* function. Finally, the prediction axes label will be named "*Probability of Spalling occurrences*" by applying the *funlable ()* function. This axis shows the probability of spalling in a concrete mixture (when it is close to zero, it means that the concrete mixture is likely to spall, and the opposite when it is close to unity). In the last stage, the nomogram is plotted using the generic *plot ()* function with the following parameters to ensure an eligible nomogram.

***R* code:**

```
>plot(nom, label.every=0.5,
 force.label=FALSE,
 xfrac=0.3, cex.axis=0.7,cex.var =0.66 , col.grid=gray(c(0.8, 0.95)),
 varname.label=FALSE, varname.label.sep='=', ia.space=0.2,
 tck=4, tcl=0.35, lmgp=0.25,
 points.label='Points', total.points.label='Total Points',
 total.sep.page=FALSE, cap.labels=TRUE)
```

Appendix C

This appendix outlines the developed web app to provide designers and practitioners a more readily access to our approach to predicting spalling.

Shiny is one of the *R* programming language packages that assist app developers in designing web-app quickly and straight. This web app consists of two main sections: 1) User Interface and 2) Server. In the first section, different slide bar panels are defined to help the app accept all the input variables in the problem (say water/binder or Heating rate) that consist of some features, including minimum, maximum, and value. On the server part, the central segment for model prediction, the

This is a preprint draft. The published article can be found at: https://doi.org/10.1007/s10694-022-01290-7.

Please cite this paper as:

Tapeh, A., Naser, M.Z. (2022). Discovering Graphical Heuristics on Fire-induced Spalling of Concrete through eXplainable Artificial Intelligence. *Fire Technology*. https://doi.org/10.1007/s10694-022-01290-7.

same logistic coefficients derived from the LR are used (Please see Fig 6 to see the half main part of the framework app).

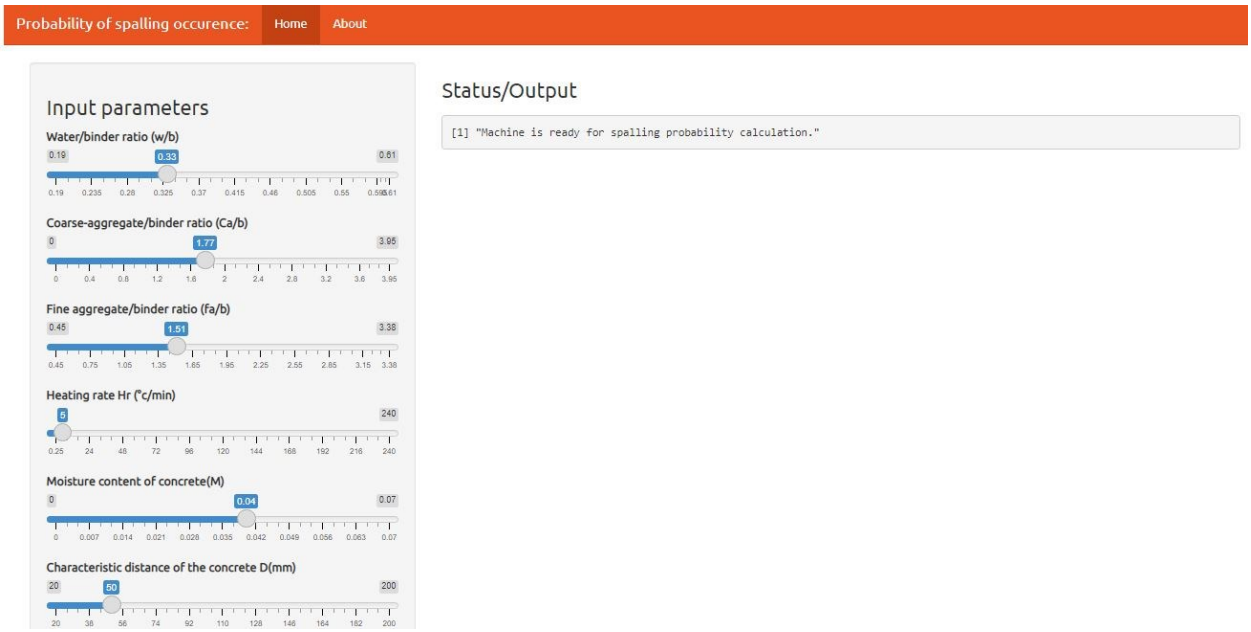

Fig. 6 Demo App (Used to predict Spalling phenomena as a new graphical user interface)

Web- app can be reached at:
https://arashteymorigharahtapeh.shinyapps.io/noto/?_ga=2.59172333.1764480149.1650622370-772174619.1645432204.